Flexible nanofilms coated with aligned piezoelectric microfibers preserve the contractility of cardiomyocytes

*P. José Gouveia [#,##], S. Rosa [#], L. Ricotti [§], B. Abecasis [§§], H. V. Almeida [#], L. Monteiro [#], J. Nunes ‡, F. Sofia Carvalho [#,##], M. Serra[§§], S. Luchkin ††, A. Leonidovitch Kholkin ††, P.Marques Alves[§§] , P. Jorge Oliveira [##], R. Carvalho [##]†, A. Menciassi [§], R. Pires Neves[#], L. Silva Ferreira * [#]*

CNC-Center of Neurosciences and Cell Biology, University of Coimbra; 3004-517 Coimbra, Portugal
Instituto de Investigação Interdisciplinar, University of Coimbra, Casa Costa Alemão - Pólo II, Rua Dom Francisco de Lemos, 3030-789, Coimbra, Portugal.
§ The BioRobotics Institute, Scuola Superiore Sant' Anna, Viale Rinaldo Piaggio 34, 56025 Pontedera (PI), Italy
§§ Inst. de Tecnologia Química e Biologica António Xavier, New University of Lisbon, Av. da Republica, 2780-157 Oeiras, Portugal
† Department of Life Sciences, Faculty of Sciences and Technology, University of Coimbra, 3000-456 Coimbra, Portugal
†† CICECO - Materials Institute of Aveiro & Physics Dept, University of Aveiro, Campus de Santiago, 3810-193 Aveiro, Portugal.
‡ Centre for Mechanical Engineering, University of Coimbra, Coimbra, Portugal; 3030-788 Coimbra, Portugal
* Corresponding author (Email:Lino@uc-biotech.pt)

KEYWORDS: cardiac tissue engineering, nanofilms, electrospun fibers, piezoelectric materials, cardiotoxicity

ABSTRACT

The use of engineered cardiac tissue for high-throughput drug screening/toxicology assessment remains largely unexplored. Here we propose a scaffold that mimics aspects of cardiac extracellular matrix while preserving the contractility of cardiomyocytes. The scaffold is based on a poly(caprolactone) (PCL) nanofilm with magnetic properties (MNF, standing for magnetic nanofilm) coated with a layer of piezoelectric (PIEZO) microfibers of poly(vinylidene fluoride–trifluoroethylene) (MNF+PIEZO). The nanofilm creates a flexible support for cell contraction and the aligned PIEZO microfibers deposited on top of the nanofilm creates conditions for cell alignment and electrical stimulation of the seeded cells. Our results indicate that MNF+PIEZO scaffold promotes rat and human cardiac cell attachment and alignment, maintains the ratio of cell populations overtime, promotes cell-cell communication and metabolic maturation, and preserves cardiomyocyte (CM) contractility for at least 12 days. The engineered cardiac construct showed high toxicity against doxorubicin, a cardiotoxic molecule, and respond to compounds that modulate CM contraction such as epinephrine, propranolol and heptanol.

1. Introduction

Several scaffolds that mimic the architecture and biophysics of the myocardium's extracellular matrix (ECM) have been proposed in the last decade, with the aim of generating engineered cardiac tissue [1-3]. Most of the cardiac tissue engineering approaches have used preformed scaffolds based on polymers such as poly(glycerol sebacate) [4] and macroporous nanowire electronic scaffolds [5], as well as hydrogels, including alginate [6], fibrin [7], tropoelastin [8] and collagen [9]. These scaffolds have impact in cardiac cell attachment/alignment, electrical signal propagation and cell maturation. Cardiac cells respond to scaffold stiffness and topographical cues by changing their cytoskeleton and morphology [10, 11]. Therefore, scaffolds that favour cardiac cell alignment have been shown to improve cell-cell interaction and tissue cohesion [11] as well as action potential duration and transient calcium direction [12]. On the other hand, scaffolds that favor electrical signal propagation between cardiac cells lead to a cardiac tissue construct that has synchronous contraction and shows high levels of proteins involved in muscle contraction and electrical coupling [6, 13]. Moreover, external electrical fields applied to scaffolds seeded with cardiac cells originate tissue constructs with higher maturation [14, 15]. In this case, the number [14] and organization [15] of mitochondria between myofibrils is higher, however, the cell's metabolic profile has not been evaluated. Overall, although the molecular mechanisms behind the inductive properties of scaffolds in cardiac biology are only partially understood, it is expectable that scaffolds that couple mechanical, anisotropy and electric properties may foster the development of a functional cardiac tissue [16].

Engineered cardiac tissue may be a relevant platform for cardiotoxicity and drug screening studies. Cardiotoxicity assessment is of paramount importance in the development of new drugs. Cardiac toxicity has been implicated in 28% of drug withdrawals over the last 30 years [17] and it represents one of the most stringent exclusion criteria in the licensing process

[18]. Although the use of CMs in a culture dish or within microfluidic systems [19] has been reported, the use of engineered cardiac tissue for automatized high-throughput drug screening/toxicology assessment remains largely unexplored. One example has been reported which encompasses a miniaturized and automated method based on engineered heart tissue [20]. Unfortunately, more than 20% of the cardiac cells died over a period of 3 days and the variability in the force and frequency between cardiac constructs was relatively high. The development of engineered cardiac tissue for drug screening requires the creation of scaffolds that are easy to produce and miniaturize, flexible, and able to preserve the contractility of CMs, ideally in the absence of an external electrical stimulation since it will facilitate its implementation in any laboratory.

Here we propose a scaffold that mimics some aspects of cardiac ECM (**Supplementary Fig. 1A**) while preserving for at least 12 days the contractility of fetal rat and human CMs derived from pluripotent stem cells. The scaffold is based on a PCL nanofilm (MNF) coated with PIEZO microfibers of poly(vinylidene fluoride–trifluoroethylene) (PVDF-TrFE). When a mechanical force is applied to a piezoelectric material a change in the polarization density occurs, due to the shifting or rotation of the constitutive dipole crystals. As a result, a transient electric charge is generated. Therefore, PIEZO fibers may act as sinoatrial node cells, which in the native tissue are responsible for cardiac pacemaking [21]. We hypothesize that (i) the MNF provides a flexible support for cell contraction and (ii) the aligned PIEZO fibers deposited on top of the MNF create conditions for cell alignment and electrical stimulation of the seeded cells.

2. Materials and methods

2.1 Preparation and characterization of MNF and MNF+PIEZO scaffolds

2.1.1 Preparation of MNF and MNF+PIEZO scaffolds. MNFs were prepared by the combined use of a sacrificial layer and spin coating [22]. Initially, a solution of PVA (1% w/v, in water; 1 mL; Mw = 25.000, 88% hydrolysed; Polysciences, Inc) was added to the surface of a silicon wafer (400 μm thick, 2 × 2.5 cm; Primewafers) and spin-coated (Spincoat G3P-8, Pi-Kem) at 4000 rpm for 20 s. Then a suspension of superparamagnetic magnetite/maghemite nanoparticles (10 mg/mL; EMG1300; diameter of 10 nm; FerroTec Co., USA) suspended in a PCL solution (20 mg/mL in chloroform; Mw=80.000, Aldrich) was added to the wafer and spin-coated according to the previous spinning parameters. For MNF experimental group, the polymer-coated wafer was immersed in water, the PVA sacrificial layer was dissolved, releasing a freely suspended insoluble nanofilm. For MNF+PIEZO experimental group, the polymer-coated silicon wafers were fixed to a home-made rotating collector for the deposition of aligned fibers (rotator motor: Heidolph RZR2020; rotative collector was made as an aluminium circular frame with the following measurements: 100 mm of diameter, 18 mm of thickness). The fibers were generated from a solution of poly(vinylidene fluoride–trifluoroethylene) (70:30 w; Solvay) dissolved in methylethylketone (Labor Spirit) according to a methodology described elsewhere [23]. The parameters used were: 10-12 kV voltage, 20% (w/v) polymer solution concentration, 12 cm tip-to-collector distance, 2 mL/h injection rate, 40-50% relative humidity at room temperature and 2.000 rpm collector's rotation speed. The selected collection time was 4 min.

2.1.2 Scaffold characterization: AFM analyses. Imaging was performed with a Bruker Innova Scanning Probe Microscope (Bruker) in dry state, operating in tapping mode, with oxide-sharpened silicon probes (RTESPA-CP, Veeco Instruments Inc.) at a resonant frequency of 300 kHz. The sample was scanned across the edge of the scratch over a 50 μm ×

50 μm area, recording 128 × 128 samples. The resulting scan data were elaborated using the Gwyddion SPM analysis tool (http://gwyddion.net). Scan data were leveled with the facet level tool to remove sample tilt, and then the film thickness was evaluated as the difference between the average heights of a region of interest (ROI) selected on the nanofilm surface and the average height of the ROI on the silicon wafer.

2.1.3 Scaffold characterization: mechanical tests. Mechanical properties were evaluated by measuring their strain in response to an applied unidirectional stress. An INSTRON 4464 Mechanical Testing System was used, equipped with a ±10 N load cell. Traction tests were performed on ten samples for each sample typology. The nanofilms were detached from the substrate, by immersing them in water, then gently fished up and allocated between two aluminium clamps. All specimens were pulled at a constant speed of 5 mm/min, until reaching sample failure. Data were recorded at a frequency of 100 Hz. The stress was calculated as the ratio between the load and the cross-section area of a tensile specimen, while the strain was calculated as the ratio between its extension and its initial length. The Young's modulus for each tested sample was extracted from its stress/strain curve.

2.1.4 Scaffold characterization: SEM analyses. A Phenom Pro tabletop SEM was used for analyses. At least 3 images were taken per each sample. Fiber diameter was determined by ImageJ software on SEM images. Fiber anisotropy was determined by a protocol described elsewhere [24] on SEM images. In this case, the orientation and anisotropy of fibrillar structures in SEM images was calculated using the image analysis software ImageJ, where computation on the basis of the gradient of pixel intensity level is performed over a region of interest in the image.

2.1.5 Scaffold characterization: assessment of impedance and the direct piezoelectric effect. Scaffold impedance spectra were analyzed by using an impedentiometer (Agilent) in the 40 Hz – 20 kHz frequency range. The capacity of piezoelectric microfibers to generate

charge (direct piezoelectric effect) was determined using a custom designed flexible gold electrodes connected to a mix signal oscilloscope (InfiiVision, Agilent Technologies). Deformation of the PIEZO microfibers was performed on the surface of two Delrin cylinders having two different curvatures: curvature I- 84 mm cylinder diameter and curvature II – 105 mm cylinder diameter. A stack of PIEZO microfibers was prepared (mass of the PVDF-TFRE fiber layer stack = 4.4 mg), and a flexible polyethylene thin-film was used as non-piezoelectric control condition (mass of control thin-film = 7.8 mg). The samples were placed in contact with the flexible gold electrodes. Next, this setup was fixed on cylinders and manually pressed repeatedly against the cylinder's surface for a short period of time. Variations of charge generation were registered during this period. At least 10 replicate measurements were performed per cylinder. The total voltage generated during each period of stimulation was calculated and normalized by the mass of sample and overall time of stimulation.

2.1.6 Scaffold characterization: PFM measurements. PFM measurements were performed using a Ntegra Prima scanning probe microscope (NT-MDT, Russia). All measurements were done using conductive TiN coated cantilevers NT-MDT FMG01/TiN (resonance frequency of the used cantilevers was 70 - 75 kHz). Topography mapping was done in a tapping mode. PFM was performed in the contact mode by placing a tip at certain points without scanning. Driving AC voltage with 150 kHz frequency and in the range 1÷10 V (amplitude) was applied to the tip under ambient conditions. Pt coated Si was inserted between the film and the substrate and served as a grounded bottom electrode.

2.1.7 Scaffold characterization: degradation tests. Samples (average sample area of 4 cm^2) were placed in PBS for 12 days at 37° C in the presence of trypsin (20 ng/mL) and collagenase type II (350 μg/mL). The enzymatic solution was replaced each three days by a fresh one. Both enzymes have been used for heart tissue digestion and isolation of primary

cells (see below). Samples without any treatment (i.e. after preparation) were used as control. Both samples were washed with PBS, lyophilized and mass assessed by weighting (and normalized the corresponding initial area).

2.1.8 Scaffold characterization: finite element model simulations. FEM simulations were performed with Matlab®R2013a (MathWorks) and Abaqus 6.13 (Dassault Sys-temes) software's. Matlab was used to design the system in a parametric way and to manage data, while Abaqus was used to perform FEM simulations. Simulation conditions for the layer used in the model were retrieved from experimental data of MN+PIEZO scaffolds, i.e. thickness of 4.5 μm and an elastic modulus of 5 MPa. Cell related conditions contained experimental data extracted from fluorescence image analysis, which provided the total value of 306 cells per area of layer, and defined the cell dimensions and distribution configurations. After creating the substrate in the Abaqus environment ($1.4 \times 1.4 \times 0.0045$ mm^3), by using the Python language, experimental data (stress-strain curves) of the MNF+PIEZO scaffold were imported by exploiting the Hyperplastic module supported by the program. In the Abaqus Step module, an explicit dynamic behavior was defined. Appropriate fixed constraints were applied to the four membrane edges, thus resembling the real situation (Fig. 1A). A quad element-based mesh was implemented with 10 μm as characteristic dimension. Cells were modelled with 40×40 μm^2 squares, spaced of 40 μm each other and anisotropically oriented along one preferential direction (data extracted from fluorescence images of the tissue constructs). Cell contraction force and orientation angle were extracted from literature data, which indicate a stress of 4 mN/mm^2 for primary cardiomyocytes [25] and an angle of ~ 20° between focal adhesion average axis and the substrate plane [26]. Von Mises stresses and overall displacement values were recorded for each simulation.

2.2 Cell culture in MNF and MNF+PIEZO scaffolds

2.2.1 Isolation and culture of rat fetal CMs. Fetal CMs were obtained from Wistar rat fetus (17-18 days of gestation) sacrificed according to the European Union directives. After sacrifice the hearts were removed, the atria were excised and the ventricles were placed in Hank's Balanced Salt Solution (HBSS, pH 7.4, Ca^{2+} and Mg^{2+} free, Sigma). Next, the ventricles were placed in a new Petri dish (30-40 per plate) containing a trypsin-EDTA solution (0.1%, w/v, Gibco) and maintained at 4ºC overnight for digestion. After 18 h, the partially digested tissues were brought to 30-37ºC and type II Collagenase (75 U/mL, Worthington Biochemical Corporation, USA) was added for 30-45 min. The digested tissue was mechanically dissociated and filtered through a cell strainer (40 μm, nylon; Falcon). After centrifugation (1200 rpm, 5 min) cells were resuspended in Dulbecco's modified Eagle's medium (DMEM) supplemented with 10% (v/v) fetal bovine serum (FBS), 100 IU mL^{-1} penicillin and 100 μg mL^{-1} streptomycin. Afterwards, the cell suspension was then purified by plating the cells in a 1% (w/v) gelatin-coated plate for 3 h. The non-adherent cells were then counted and platted at a density of 450.000 cells per scaffold (effective area of the scaffold is 0.8 cm^2) in DMEM supplemented with 10% (v/v) FBS, 100 IU mL^{-1} penicillin and 100 μg mL^{-1} streptomycin. The average cell yield was of 130×10^4 per heart.

2.2.2 Differentiation of human induced pluripotent stem cells (iPSCs) into CMs. Human iPSCs DF19-9-11T.H (WiCell, Madison, WI) were cultured on Matrigel® hESC-Qualified Matrix (Corning, NY, USA) coated plates in mTeSR1 medium (StemCell Technologies, Vancouver, Canada) until reaching 80% confluence. CM differentiation was induced as described by Lian *et al*. [27]. At day 15 of differentiation, 2D monolayer cultures composed by 85-99% of hiPSC-CMs (characterized by the expression of cardiac troponin T and SIRPA using flow cytometry analysis, as described in section "FACS analysis") were obtained. For the experiments with nanofilms, monolayer cultures were dissociated into single cells at this time-point, by incubation with TrypLE™ Select (Thermo Fischer Scientific) for 5 min,

centrifuged (220g, 5 min) and resuspended in standard CM culture medium (RPMI supplemented with B-27 minus insulin, both from Thermo Fischer Scientific).

2.2.3 Phenotype characterization of cardiac cells by FACS analyses. For the experiments with cells of rat origin, cardiac cells after isolation (see protocol above; 1.25-2.5 × 10^5 cells per condition) were fixed in 4% (v/v) paraformaldehyde (Electron Microscopy Sciences) solution for 15 min and then washed two times with PBS. Cells were then permeabilized with saponin (0.5%, Sigma) and labelled with antibodies against cardiac fibroblasts (anti-vimentin, rabbit, Abcam), CMs (anti-α-actinin, mouse, Sigma) or endothelial cells (anti-CD31, mouse, ThermoFisher Scientific). After a washing step, cells were characterized by a FACS Calibur (BD) and the data analyzed by a Cell Quest software. Twenty thousand events were collected in each run. For the experiments with human CMs, after a 5 min dissociation with TypLE™ Select, hiPSC-CMs were washed twice with PBS and a total of 5×10^5 cells were incubated with conjugated antibody SIRPα/β (CD172a/b-PE, BioLegend) or isotype control IgG1,κ-PE (BD Biosciences) for 1 h at 4°C. For analysis of the expression of cardiac Troponin T, cells were fixed and permeabilized with Cytofix/CytoPerm kit (BD Biosciences) according to the manufacturer's instructions, and incubated with the primary antibody cardiac Troponin T (Thermo Fischer Scientific) or isotype control IgG1 (Santa Cruz Biotechnology) for 1 h at 4°C. Cells were washed twice with DPBS, and incubated with the secondary antibody Alexa Fluor® 488 Goat Anti-Mouse IgG (Thermo Fischer Scientific). After two washing steps with PBS, cells were analysed in a CyFlow® space (Partec GmbH) instrument, registering 10.000 events/sample.

2.2.4 Co-culture of human cells. Normal human dermal fibroblasts (Lonza) were cultured in DMEM supplemented with 10% (v/v) FBS, 100 IU mL^{-1} penicillin and 100 μg mL^{-1} streptomycin. After cell confluence, they were dissociated into single cells by incubation with trypsin-EDTA solution (0.1%, w/v, Gibco) for 5 min. After centrifugation (1200 rpm, 5 min),

fibroblasts were resuspended in RPMI supplemented with B-27 minus insulin and seeded with hiPSC-CMs (ratio of 5:1 CM:Fibroblasts). This co-culture was platted with a cell density of 600.000 cells per scaffold in RPMI supplemented with B-27 minus insulin (Thermo Fischer Scientific).

2.2.5 Coating of the scaffolds for cell culture. The scaffolds were coated with poly(dopamine) and then with a gelatin solution (1%, w/v). The poly(dopamine) coatings were prepared as described by Haeshin Lee *et al.*[28]. Briefly, scaffolds were immersed in a dopamine solution (2 mg of dopamine/HCl per mL of 10 mM Tris buffer pH 8.5) typically overnight and rinsed with water for further use. The scaffolds were afterwards mounted in a Cellcrown (Scaffdex Oy, Finland) before cell seeding. Next, the structures were sterilized while immersed in a disinfection solution of Penicillin-Streptomycin (1000U/mL, Life Technologies) and amphotericin B (Fluka, 10 µg/mL) for 24 h. Afterwards, the nanofilms mounted in Cell Crowns were exposed to UV light for 30 min and stored at 4°C. Prior to cell culture, the antibiotics/amphotericin solution was removed and the supports were coated with a 1% gelatin in solution for 12 h.

2.3 Characterization of engineered cardiac tissue

2.3.1 Cell adhesion analyses: DNA extraction and total DNA quantification. DNA samples were obtained from cell extracts with TRIzol Reagent (Invitrogen). Extraction was performed accordingly to protocol described by the manufacturer. Total cell extracts were divided into 3 different phases containing respectively RNA, DNA and protein. Quantification of each component was performed by NanoDrop.

2.3.2 Cell proliferation and viability tests. For the assessment of cellular proliferation and viability two different methods were performed: MTT assay (thiazolyl blue tetrazolium bromide, Sigma) and PrestoBlue (Invitrogen). In case of MTT assay, the cells were incubated

with medium (DMEM, Biochrom) supplemented with MTT (5 mg/mL) for 1 h. Then, cells were washed with PBS and DMSO was added for 20 min so that the MTT salts could be solubilized. After a centrifugation step the absorbance of the supernatant was read at 540 nm and 620 nm. For the PrestoBlue, cells were incubated for 2 h and 30 min with a 10% solution of the reagent and medium. The resulting supernatant was diluted (1:1) with medium and fluorescence measured at excitation 535 nm and emission 615 nm.

2.3.3 Cell characterization: immunocytochemistry analyses. At specific time points, cells were fixed in 4% (v/v) paraformaldehyde for 10 min and permeabilized with 0.1% (v/v) Triton or with methanol for 10 min when it was recommend by the antibody supplier. Following the blocking step with 1% (w/v) BSA for 30 min the cells were incubated with the primary antibody for 1 h at room temperature. The primary antibodies used were: anti-vimentin (rabbit, Abcam), anti-α-actinin (mouse, Sigma), anti-connexin 43 (rabbit, Sigma), anti-troponin I (goat, Santa Cruz) anti-calsequestrin 2 (goat, Santa Cruz), anti-dihydropyridine receptor alpha-1 (mouse, Thermo Scientific), hERG (rabbit, Santa Cruz). After extensive washes with PBS cells were incubated with the secondary antibody for 30 min at room temperature and counterstained with DAPI. Cellular alignment was quantified on confocal microscopy images taken on samples (63×) labelled for α-actinin (mouse, Sigma; CM population), vimentin (rabbit, Abcam; CF population) and DAPI (cell nucleus). Each image was processed according to an analysis protocol described elsewhere [24]. The orientation and anisotropy of fibrillar structures in raw images was done using the image analysis software ImageJ, where computation on the basis of the gradient of pixel intensity level is performed over a region of interest in the image.

Fluorescence intensity analysis was performed while using ImageJ image analysis tool set. Briefly, a region of interest (ROI) was selected by using a drawing/selection tool. Next, measuring settings “Area”, “Integrated density” and “Mean grey value” were selected

at the “Analyse - Set measurements" menu. Measurements were done for the ROI and for the respective background levels (3 measurements per image). Afterwards, the measured values were used to calculate the corrected total cell fluorescence (CTCF) as follows:

$$CTCF = Integrated\ Density - (Area\ of\ ROI\ X\ Mean\ Fluorescence\ of\ background)$$

2.3.4 Cell characterization: western blot analyses. Cell protein extracts were diluted in SDS sample buffer (2.5% SDS, 0.0625 M Tris-HCl, 10% glycerol, 5% 2-mercaptoethanol, 0.05% bromophenol blue, pH 6.8) and boiled for 5 min at 95ºC. Proteins (30 μg) were separated by SDS/PAGE [10% (v/v)] and transferred onto PVDF membranes by electroblotting. The membranes were blocked with 5% skim milk in Tris-buffered Saline-Tween (TBS-T, 20 mM Tris-HCl, 150 mM NaCl, 0.1% Tween 20) and then probed with an antibody for connexin 43 (produced in rabbit, Sigma), for troponin I (produced in goat, Santa Cruz) or for α-actinin (produced in mouse, Sigma). After extensive washings with TBS-T, the blots were incubated with an alkaline phosphatase-conjugated secondary antibody (GE Healthcare, Buckinghamshire, UK). Immunoreactive complexes were detected by chemifluorescence using the ECF reagent (GE Healthcare). Fluorescence was detected with a Molecular Imager FX scanner (Biorad). To ensure an equal protein loading, antibody for CsQ2 (Santa Cruz) was used as internal control. The intensity of the bands was analyzed using the TotalLab TL120 software (Nonlinear Dynamics).

2.3.5 Cell characterization: quantitative real-time PCR (qRT-PCR) analyses. For the *in vitro* conditions, total RNA was extracted with TRIzol Reagent (Invitrogen) and immediately stored at -80ºC. In the case of the *in vivo* rat samples extraction of the RNA samples from the collected heart tissue was performed with an RNA extraction kit (Qiagen). In case of human cell experiments, Human Heart Total RNA (Clontech) extracts were used as reference. RNA was quantified in a NanoDrop ND-1000 Spectrophotometer (NanoDrop Technologies, Inc.,

USA) at 260 nm. The cDNA was reverse transcribed from 1 μg of total RNA, using TaqMan Reverse Transcription Reagents kit (Invitrogen) according to the manufacturer's instructions. The cDNA obtained was stored at -20ºC until further analysis by real time PCR using the fluorescent dye SYBR Green and the 7500 Fast Real Time PCR System (Applied Byosystems). Specific sets of primers were designed by SIGMA (see supplementary Table 1). Quantification of target genes was performed relative to the reference CsQ2 or TBP (TATA box binding protein). Genes relative expression= $2^{[-(Ct_{sample} - Ct_{reference})]}$. The mean minimal cycle threshold values (Ct) were calculated from quadruplicate reactions.

2.3.6 Cardiac activity: beating analyses. Videos of the samples were recorded (Camstudio) using a light microscope at a magnification of 20×. The videos had an average of 300×300 pixels of area. One recording was performed per replicate per experiment. These recording focused on a hot spot, i.e., an area where synchronous beating was clearly visible. The number of beatings was obtained by manually counting each beat during the time span of the videos. It is important to note that since the resolution of the recorded videos was low it was not possible to use automatic imaging processing methods.

2.3.7 Cardiac activity: live cell Ca^{2+} analyses. Acquisitions were performed in a Spinning Disc Confocal (Carl Zeiss). Intracellular Ca^{2+} transients were quantified with a Fluo-4 probe (Life Technologies) in cardiac cells cultured in MNF+PIEZO scaffold for 12 days. Firstly, cells were washed twice with HBSS buffer. Then, cells were incubated in the dark, at room temperature, for 30–60 min with a loading buffer (PowerLoad™, Probenecid and probe, Life Technologies). Afterwards, the cells were washed with cell culture media (RPMI supplemented with B-27 minus insulin, Thermo Fischer Scientific) and kept in the same media during live recording. In the pharmacological tests the constructs were incubated with the target compounds for at least 5 min before acquisition.

Analysis of the fluorescence intensity was performed for each frame of the live recording. Fluorescence intensity analysis was performed with the ImageJ image analysis tool described previously (see Immunocytochemistry analysis). The function used in the Ca^{2+} flux profiles was "Plot Z-axis Profile". Results are shown by fluorescence intensity as a function of time (acquisitions of 60s, total of 342 frames). Due to photobleaching decay occurring during recording, the resulting videos were adjusted by using a custom ImageJ's macro. Briefly, this macro calculates the decay rate of a bleached ROI over time and normalizes the fluorescence of each video frame against the intensity of the previous one. Afterwards, the values of fluorescence intensity obtained were normalized by the respective baseline intensity.

A representative video was selected from each tested condition. The profiles for the condition without compounds, with epinephrine (Sigma) and with propranolol (propranolol hydrochloride, Sigma) are the average of 3 independent ROIs from each respective video recording. The profiles for the heptanol condition show the intracellular Ca^{2+} fluxes of 3 separated ROIs measured from the same video acquisition.

2.3.8 Cardiac activity: metabolic profile as evaluated by nuclear magnetic resonance (NMR). Cells were cultured in Dulbecco′s Modified Eagle′s Medium (D5030, Sigma) supplemented with 1.0 g/L [1,6-^{13}C2]glucose (Cambridge isotopes), 0.584 g/L L-glutamine (Life Technologies), 3.7 g/L sodium bicarbonate (Sigma) and 10% FBS (Alfagene). ^{1}H-NMR spectra were acquired in a 600 MHz Varian VNMRX spectrometer using a 3 mm broadband NMR probe. Each NMR spectrum consisted of 32k points covering a sweep width of 7.2 kHz. An interpulse delay of 10 s and a 45° radiofrequency reading pulse were used to ensure full relaxation of all nuclei in the sample. A total of 16 scans were averaged to ensure adequate signal to noise for quantitative purposes. Before Fourier transformation, the free induction decay (FID) was multiplied by a 0.2 Hz Lorentzian apodization function. NMR

spectra deconvolution was achieved by NUTSproTM NMR software using the line-fitting subroutine which allows deconvolution of individual lines. Each NMR sample consisted of 20 μL culture media plus 200 μL of a 2.5 mM sodium fumarate (internal standard) phosphate buffered D2O (99.9%) solution.

2.4 *In vivo* testing. The sub-chronic animal model was performed in Wistar rats (8 weeks old) assigned to 2 groups: DOXO and Vehicle [29]. In this case, animals were injected subcutaneously weekly in the scruff or flank with 2 mg/Kg DOXO or with equivalent volume of vehicle solution (0.9% NaCl), during 7 weeks. At the end, animals were allowed to rest for 2 weeks before being sacrificed. Animals were euthanized by cervical dislocation followed by decapitation, confirming death of the animal. Extraction of the heart with the aortic stump from the thorax was quickly performed, and heart was washed in a cold (4ºC) Tyrode´s buffer to remove blood. For mRNA analyses, heart tissues were preserved in RNAlater solution (Ambion, Austin, USA) following the manufacturer's instructions.

2.5 Statistical analyses. An unpaired *t* test or one-way ANOVA analyses of variance with Bonferroni/Newman-Keuls post-tests were performed for statistical tests using GraphPad Prism. Results were considered significant when $P < 0.05$.

3. Results and discussion

3.1 Preparation and characterization of MNF+PIEZO scaffolds. To prepare the nanofilms, PCL dissolved in chloroform was spin-coated on silicon wafers previously coated with a sacrificial layer of poly(vinyl alcohol) (PVA) (**Fig. 1A**). Because these nanofilms are fragile and difficult to manipulate in aqueous solutions, superparamagnetic nanoparticles

(SPIONs) were added to the PCL solution before the spin coating as described elsewhere [22]. The resulting nanofilm has magnetic properties, thus facilitating manipulation of the nanofilm by using an external magnet (**Supplementary Movie 1**), and displays similar mechanical properties to nanofilms without SPIONs (**Supplementary Fig. 1E**). We employed PCL to generate the nanofilms due to its elasticity, biocompatibility, and a long history in biomedical applications [30]. In addition, it is expected that the low degradation rate of PCL will not interfere with the *in vitro* maintenance of the cardiac tissue (**Supplementary Fig. 1F**).

For the preparation of nanofilms we screened different concentrations of PCL, with the aim of yielding a stable ultrathin polymeric film with low elastic modulus (**Supplementary Figs. 1B-1D**). After this screening process, we prepared a nanofilm with an area of 2×2.5 cm^2, an approximate average thickness of 229 nm as measured by atomic force microscopy (AFM), an average surface roughness (Ra) of 0.09 ± 0.03 μm as measured by AFM and an elastic modulus of 0.06 ± 0.04 MPa as evaluated by traction test (**Fig. 1B.1**). The resulting free-standing nanofilm is brownish (due to the presence of SPIONs), very flexible and can be manipulated with tweezers or by using a magnet (**Supplementary Fig. 1B**).

To prepare PIEZO microfibers, a solution of PVDF-TrFE (20%, w/v) was electrospun. This copolymer was chosen because it has enhanced spontaneous dipolar orientation after electrospinning [31] and it has excellent biocompatibility properties [32, 33]. Electrospinning conditions were optimized to generate fibers with relatively low diameter and high anisotropy after deposition onto the MNF (scaffold named as MNF+PIEZO) (**Supplementary Fig. 2**). In the tested conditions (**Figs. 1C, 1D and Supplementary Fig. 2B**), porous fibers with a diameter of 1.24 ± 0.13 μm (average ± SEM, n=3) were obtained. These fibers have piezoelectric properties as determined by piezo-response force microscopy

(PFM), a local probe-based technique for non-destructive high-resolution piezoelectric domain imaging and manipulation [34]. Following the topography acquisition in tapping mode, the AFM was switched to the PFM in which the conducting tip was scanning in contact mode while an *ac* voltage (V_{ac}) was applied between the tip and Au electrode (**Figs. 2A.1 and 2A.2**). Over different points of the fibers, the surface amplitude of the piezo-response varied between 3.5 ($d_{33(min)}$) and 11.1 pm/V ($d_{33(max)}$) (**Fig. 2A.3).**

The MNF+PIEZO scaffold showed an average surface roughness (Ra) of 1.30 ± 0.06 μm as measured by AFM (**Fig. 1D**) and an elastic modulus of 5.08 ± 0.82 MPa (average ± SEM, n=3) as measured by tensile tests (**Fig. 1B and Supplementary Fig. 1E**), showing that the presence of the PIEZO fibers led to mechanically stronger constructs than MNF alone. Impedance measurements were also performed to evaluate both the piezoelectric and conductive properties of the constructs. The results demonstrate that the MNF scaffold has stable impedance values for all frequencies, while MNF+PIEZO scaffold shows a spectrum with two peaks, a resonance (f_R) and an anti-resonance frequency (f_A) (**Fig. 1E**), typical of piezoelectric materials [35]. To further evaluate the charge generation capability by the piezoelectric fibers, mechanical deformation tests were performed (**Fig. 2B.1**). Measurements were accomplished by using a custom designed flexible gold electrode coupled to a mix signal oscilloscope. Deformation of the PIEZO fiber layers was achieved by bending the substrates over the surface of Delrin cylinders featured by two different diameters, thus obtaining two different substrate deformation curvatures (curvature I – cylinders with an 84 mm diameter; curvature II – cylinders with a 105 mm diameter) (**Fig. 2B.2**). We registered a 2-fold increase (from 11.4 mV/s to 26.7 mV/s) of the charge generated with the increase of the deformation curvature.

3.2 MNF+PIEZO scaffolds enhance rat cardiac cell stratification and alignment. To evaluate the *in vitro* biocompatibility of the scaffold, primary prenatal rat cardiac cells (59.5 ± 2.9 %, CM; 32.1 ± 2.4 % cardiac fibroblasts (CF) and 5.1 ± 4.7 % endothelial cells; **Supplementary Fig. 3**) were seeded on top of the scaffolds and cultured for 12 days. We have selected prenatal rat cardiac cells for the initial screening because (i) these cells have been used in studies for cardiac scaffold design [36], (ii) their immature stage in terms of development is important to evaluate CM maturation [37, 38] and (iii) it is relatively easy to have these cells in the desired numbers, while human CMs derived from pluripotent stem cells are costly and more difficult to obtain. We selected 12 days for our analyses to allow the organization of cells in proper constructs, while being primed by the ECM for a maturation process. This time-point represents a good compromise in view of a use of this engineered cardiac tissue for drug screening by pharmaceutical industries.

MNF+PIEZO scaffolds are cardiac cell adhesive and permissive to cardiac cell proliferation. Cell adhesion evaluated by DNA quantification at day 1 showed that all the substrates have equivalent cardiac cell adhesive properties (**Supplementary Fig. 3**). Because cardiac fibroblasts and endothelial cells may mediate CM adhesion to the substrate we have isolated CM from the initial cardiac cells by magnetic cell sorting and perform the same adhesion tests. Again, similar adhesion results for all the substrates were observed. In addition, cell proliferation evaluated by DNA quantification for the first 3 days showed that cardiac cells proliferate in the scaffolds and the proliferation rate was higher for cells seeded in MNF or MNF+PIEZO scaffolds than in tissue culture poly(styrene) (PS). Moreover, MTT results showed that cells proliferated from day 1 to day 12 (**Fig. 3A**).

We then asked whether the cell population on the scaffold was altered over time. CMs and CFs were identified by the expression of α-actinin and vimentin, respectively (**Fig. 3B**). At day 1, approximately 75% of the cells were CM and only 25% were CF (slight variations

in this ratio were observed between the different experimental conditions). This cell ratio was not statistically different at day 12. Altogether, our results show that MNF+PIEZO scaffolds support cell adhesion and proliferation and maintain the CM/CF ratio from day 1 to day 12. These results compare favourably to previous studies showing a detrimental decrease in CM population overtime when cultured in different scaffolds [39, 40].

MNF+PIEZO scaffolds but not MNF or PS enhanced cellular stratification. At day 12 (T12), CMs were located in the proximity of the fibers of the MNF+PIEZO scaffold, while CFs were located on top of CMs and therefore distant from the PIEZO fibers (**Supplementary Fig. 4**). It has been shown that cells respond differently to the microtopography [41] and stiffness [42] of the substrates. An attractive possibility is that this stratification is linked to the piezoelectric properties of the fibers. Indeed, their capacity to generate electrical charge may constitute a source of tropism for CMs.

Previous studies have shown that cell alignment is of utmost importance to generate contractile cardiac-like tissue. For example, CM aligned by the use of micro- and nanopatterned biomaterials show higher action potential conduction velocity and express higher levels of cell-cell coupling proteins such as Cx43, in comparison with randomly oriented CM [8, 11]. To evaluate whether MNF+PIEZO scaffolds enhanced cell alignment, the local cell alignment index was quantified by image analysis. For this purpose α-actinin and vimentin filament orientation was identified and analyzed for CM and CF populations, respectively (**Figs. 3C.1 and 3C.2**). On MNF+PIEZO scaffolds, CMs showed a 3-fold increase in alignment at day 12 as compared to day 1, while no significant alignment was observed for the other conditions (PS and MNF scaffolds) at the same time-point. CMs aligned with respect to the fibers as shown by a clear orientation of the sarcomeric α-actinin fibers along the main PIEZO fibers axis. This clearly suggests a positive impact of topography on cellular organization (**Figs. 3C.1, 3D and 3E**). Regarding the CF population,

cell alignment was poor in all conditions (**Fig. 3C.2**). Overall, MNF+PIEZO scaffolds enhanced rat CM but not CF alignment. Selective CM alignment might be ascribed to the stratification effect described above, i.e., to the proximity of CMs to the piezoelectric fibers. Although cell alignment on ultrathin polymeric films has been reported recently on poly(styrene) [43] and poly(lactic-*co*-glycolic acid) [44] nanofilms, this was achieved by the use of a poly(dimethylsiloxane) mold with microgrooved motifs. Furthermore, anisotropic cell organization has been also obtained by means of electrospun fibers alone [45, 46]. Our study is the first to report the use of electrospun microfibers on top of flexible nanofilms to control cell alignment.

3.3 MNF+PIEZO scaffolds enhance cell-cell communication and preserve CM contractility. The impact of MNF+PIEZO scaffolds in cardiac cell physiology was evaluated. For that purpose, rat prenatal cardiac cells cultured in MNF+PIEZO for 12 days was evaluated by western blot analysis for sarcomeric α-actinin, troponin I and connexin 43 (Cx43) [13, 15, 39]. The band corresponding to the phosphorylated Cx43 (pCx43), and thus active form of the protein [47, 48], was quantified and normalized by total Cx43 levels. Our results show that the ratio pCx43/totalCx43 was statistically higher (P<0.05) on CMs cultured on MNF or MNF+PIEZO scaffolds than on PS at day 12 (T12) (**Fig. 4A**). Cx43 has been shown to regulate cell-cell communication and to promote a contractile phenotype in CM [49]. The increased expression of the active form of Cx43 (pCx43) in CMs seeded on both MNF and MNF+PIEZO scaffolds indicates that both scaffolds promote cell-cell interaction. We complement the previous western blot analyses with immunostaining to evaluate the location of Cx43 (total Cx43) in the engineered cardiac tissue (**Supplementary Fig. 5**). For all the conditions tested, Cx43 was located in cell-cell contact regions. In case of

cardiac cells cultured in MNF+PIEZO scaffold the pericellular location of Cx43 in CMs followed, in many cases, the alignment of PIEZO microfibers.

To further characterize the phenotype of CMs, both sarcomeric α-actinin and troponin I protein amount was assessed by western blot and normalized by the expression of calsequestrin 2 (CSQ2), a CM specific protein [39]. No changes in sarcomeric α-actinin were observed for all the experimental conditions tested (**Fig. 4B**). An increase in troponin I was observed for cells cultured in MNF+PIEZO, although no statistical significant difference (P>0.05) was observed between the conditions tested (**Fig. 4C**). It is possible that in both cases (α-actinin and troponin I) the variation occurs in the phosphorylated forms of the proteins but not in the total levels of the proteins. For example, it is known that the phosphorylation levels of troponin I regulates its activity [50]. Moreover, previous studies have shown that contractile CMs cultured in 3D scaffolds for 12 days have similar levels of α-actinin expression to day zero [20].

Then we sought to evaluate whether MNF+PIEZO scaffolds could preserve CM contractility overtime. The frequency of heartbeats in rats is around 360 beats per min (i.e., 6 Hz) [51]. Therefore, we evaluated the number of spontaneous synchronous beatings per minute in CMs at day 1 and 12 post-cell seeding (**Fig. 4D**). While the average rate of beats on cells cultured in PS and MNF scaffolds did not vary from day 1 to day 12, a significant increase in the beating frequency was observed for cells cultured in MNF+PIEZO scaffolds (from 18 to 119 beats/min). This indicates that MNF+PIEZO scaffolds provided a better environment to preserve the spontaneous contractility of CMs than the other experimental groups. Therefore, for the subsequent experiments we focused on MNF+PIEZO scaffolds, with the aim of deeply characterizing the cell-scaffold interaction mechanisms.

To understand whether the observed contractility preservation was due to the piezoelectric properties of the fibers, we prepared another MNF scaffold having on top

aligned PCL fibers (MNF + PCL), as non-electroactive substitutes of the PIEZO ones (**Supplementary Fig. 6**). The PCL fiber-based scaffold ability to maintain CM contractility was significantly lower than the PIEZO fiber-based scaffold. In line with these results, cardiac cells cultured in PCL fiber-based scaffolds showed lower levels of Cx43 mRNA transcripts, and thus lower intercellular communication, than cells cultured in PIEZO fiber-based scaffold (**Supplementary Fig. 6E.1**). The high beating rates observed in cells cultured in MNF+PIEZO scaffolds are likely due to the positive effect of the electrically charged environment generated by the PIEZO fibers during cell contraction. Thus, to confirm this hypothesis, finite element model (FEM) simulations were performed to show that the MNF+PIEZO scaffold did undergo a significant deformation during CMs beating. Local stresses up to ~ 0.5 MPa (**Supplementary Fig. 7B.1 and 7B.2**) and displacement values up to ~ 0.2 mm (**Supplementary Fig. 7B.3**) have been registered. In addition, we have quantified the expression levels of mRNA transcript for the gene *Adss1*, which encodes a muscle-specific isoform of adenylosuccinate synthetase. It has been demonstrated that this gene is activated once CMs are electrically paced [52]. The MNF+PIEZO condition showed expression levels nearly 10 times greater than the MNF+PCL condition (**Supplementary Fig. 6E.2**) and thus showing a charge effect of piezoelectric fibers on CMs.

Altogether, the high levels of Cx43 phosphorylation indicate that cells cultured in MNF+PIEZO scaffolds have increased cell-cell communication, likely influencing electrical coupling and promoting contractile behavior, as compared to CMs cultured in PS. Similar results have been previously reported for cardiac tissues cultured under electrical stimulation or conductive scaffolds [6, 13, 15]. Our results further show a discrete increase in the expression of markers related to contractile cellular apparatus such as troponin I. Notably, the contraction frequency observed in CMs seeded on MNF+PIEZO is higher than the one observed for other constructs such as scaffolds formed by elastin (ca. 40 beats min^{-1}, day 12)

[8], methacrylated gelatin (ca. 20 beats min^{-1}, day 12) [8], methacrylated gelatin containing carbon nanotubes (ca. 45 beats min^{-1}, day 9) [53] and Matrigel with fibrin (ca. 70 beats min^{-1}, day 15; average of 6 series) [20]. Furthermore, pre-natal rat CMs cultured in MNF+PIEZO exhibit an increase in the contraction frequency overtime while cells cultured in hyaluronic acid patterned glass surfaces or Matrigel exhibit a decrease in their contraction frequency within 7 days of culture [54, 55]. It is likely that the enhanced contractility of the cardiac cells in MNF+PIEZO scaffolds is due to electric charge generated during CM contraction. During CM contraction action potential signal varies approximately 100 mV [56]. Considering the PIEZO microfiber properties, we propose that the electrical stimuli provided by PIEZO microfibers (~10-30 mV) is generated in the proximity of CMs, allowing a direct and efficient stimulation.

3.4 Engineered cardiac tissue in MNF+PIEZO scaffolds with human CMs derived from iPSCs. We extended the previous studies in rat prenatal CMs to human CMs derived from iPSCs (hiPSC-CM). hiPSC-CMs were generated and cultured as reported previously by us [57]. hiPSC-CMs were seeded on MNF+PIEZO scaffolds or in PS (as control), alone or in co-culture with human fibroblasts. A ratio of CM:fibroblast 5:1 was selected based in the CM:mesenchymal ratio present in early stages of human development (1 month after birth) [58]. In contrast to rat CMs (see before), human CMs cultured alone in MNF+PIEZO scaffolds aggregated into clusters and thus did not form a monolayer of cells (**Supplementary Fig. 8A.1**). However, human CMs co-cultured with fibroblasts in MNF+PIEZO scaffolds adhered well to the scaffold (**Fig. 5A.2 and Supplementary Figs. 8A.2 and 8B**) and proliferated overtime (**Supplementary Fig. 8B**). Importantly, as noted previously for rat prenatal CMs, human CMs were located in the proximity of the PIEZO microfibers, while fibroblasts were located on top of CMs and therefore distant from the

PIEZO microfibers (**Movie 2A**). Such cellular stratification was not observed in cells cultured in PS substrates. Our results indicate that human fibroblasts have an essential role in the adhesion and morphology of CMs seeded on the MNF+PIEZO substrate. It is known that fibroblasts greatly contribute to production and enrichment of the ECM environment, which may contribute for CM adhesion [59]. Because CM monocultures did not form a monolayer of cells in MNF+PIEZO scaffold and showed low expression of troponin T and Cx43 (**Fig. 5B**) we performed the subsequent characterization for co-cultures of CMs with fibroblasts.

The impact of MNF+PIEZO scaffolds in human cardiac cell physiology was initially evaluated for the expression of CX43 protein (total) and troponin T. CMs co-cultured with fibroblasts in MNF+PIEZO scaffolds showed a 2-fold increase in the expression of Cx43 (total) relatively to the cells cultured in PS (**Fig. 5B.1**). In addition, CM's cultured in MNF+PIEZO scaffolds expressed 3 times more troponin T levels than CMs cultured in PS (**Fig. 5B.2**).

To evaluate whether MNF+PIEZO scaffolds enhanced cell alignment, the local cell alignment index was quantified by image analysis [24]. For this purpose, α-actinin and vimentin filament orientation was analyzed for CM and fibroblasts populations, respectively (**Fig. 5E**). Both cells have higher alignment index in MNF+PIEZO scaffolds, along the PIEZO microfibers, than in PS substrate.

The average beating rate in humans is 60-70 (1 Hz) [51]. To evaluate whether MNF+PIEZO scaffolds preserve human CM contractility, the number of spontaneous synchronous beatings per minute was monitored at day 1 and 12 post-cell seeding (**Fig. 5C**). Although CMs cultured in MNF+PIEZO or PS had a significant reduction in the beating rate during the 12 days, the decrease was lower in cells cultured in MNF+PIEZO than in PS. This indicates that MNF+PIEZO scaffolds provided a better environment to preserve the spontaneous contractility of CMs than PS.

To complement the previous contractility studies, we evaluated by qRT-PCR 4 of the most relevant ion channel subunits in mammalian CM electrophysiology [48]: *CACNA1C*, *SCN5A*, *KCNQ1* and *KCNH2* (**Supplementary Fig. 9**). Human cells cultured on MNF+PIEZO showed higher content of 2 ion channel subunits (transcripts *SCN5A* and *KCNH2*) than cells cultured on PS (in rat, all 4 ion channel subunits were upregulated in MNF+PIEZO than in PS). *SCN5A* encodes an alpha subunit of voltage-gated Na^+ channel while *KCNH2* transcripts encode a voltage-activated potassium channel (hERG). Both ion channel subunits participate at different stages of action potential [60].

Altogether, our results show that cardiac cells cultured in MNF+PIEZO scaffold have higher expression of Cx43 (total) and troponin proteins, higher cell alignment, higher contractility for at least 12 days, and higher expression of some ion channel subunits than cardiac cells cultured in PS substrate.

3.5 Engineered human cardiac tissue in MNF+PIEZO scaffolds respond to cardiotoxic compounds. During early cardiac development, glycolysis is a major source (80%) of energy. However, as CMs mature, mitochondrial oxidative capacity increases and fatty acid β-oxidation (80%) becomes the major source of energy [61]. To complement the previous functional and physiological studies, we evaluated the metabolic profile of cells cultured in PS and MNF+PIEZO scaffolds for 12 days by nuclear magnetic resonance (NMR). Cardiac cells in MNF+PIEZO or PS were cultured for 24 h in media containing [1,6-$^{13}C_2$] glucose and their metabolic profiles followed by [1,6-$^{13}C_2$] glucose consumption and [3-^{13}C] lactate production (**Supplementary Fig. 10A and Fig. 6A**). The ratio of glucose consumed per lactate produced is statistically higher for cells cultured in MNF+PIEZO scaffolds than in PS or MNF+PCL scaffolds indicating a higher oxidative metabolic activity, and thus a metabolic maturation process (**Fig. 6B and Supplementary Fig. 6F**). Previous studies with engineered

cardiac tissues have shown an increase in the number of mitochondria in more mature CMs [14], however, as far as we know, metabolic studies in engineered cardiac tissues were never reported.

Next, we assessed the potential of the engineered cardiac tissue in MNF+PIEZO scaffolds to respond to cardiotoxic compounds. The drug model used was doxorubicin (DOXO), often used in the clinics to treat patients with leukemias and solid tumors. The cardiotoxic effects of DOXO have been widely reported, with mitochondria as primary target [62, 63]. DOXO impairs mitochondrial oxidative metabolism and thus cells rely on glycolysis to generate ATP. Cells cultured in MNF+PIEZO and PS for 12 days were pulsed with 500 nM of DOXO for 24 h. This concentration of DOXO is in the range of concentrations typically used in the clinic [64]. Cells were then characterized for viability and transcripts of genes related to stress responses (*BAX*, *GADD45*) (**Supplementary Fig. 11**). Our results show that cells cultured in MNF+PIEZO scaffolds for 12 days are more sensitive to the effect of DOXO than cells cultured in PS for the same time, since nearly 37% *versus* 16% of the cells died after 24 h of exposure to DOXO, respectively (**Supplementary Fig. 11A**). As expected for a cell damage process, cardiac cells cultured in MNF+PIEZO or PS showed an up-regulation in the expression of *BAX* and *GADD45* after exposure to DOXO (**Supplementary Fig. 11B**). Similar results were observed with rat cardiac cells cultured in MNF+PIEZO or PS and in cardiac cells isolated from hearts of rats that received multiple doses of DOXO over 7 weeks (see Supplementary Information and Materials and Methods for details) (**Supplementary Figs. 11C and 11D)**. Importantly, as observed with rat cardiac cells (**Supplementary Fig. 10B**), the metabolic profile of human cardiac cells cultured in MNF+PIEZO became more glycolytic after exposure to DOXO, while cells cultured in PS had similar levels of glycolysis before and after exposure to DOXO (**Fig. 6B.2**). The increase of glycolysis on cells cultured in MNF+PIEZO is consistent with mitochondrial dysfunction

elicited by DOXO. Exposure to DOXO leads to an inhibition of mitochondrial oxidative metabolism, which is likely to be compensated by glycolysis.

Overall, our viability and metabolic profiling results indicate that engineered cardiac tissues in MNF+PIEZO scaffolds respond to cardiotoxic compounds to a level that is not possible to achieve using cells cultured in regular conditions (in this case cultured in PS). The higher sensitivity of our engineered cardiac tissue is likely due to a more active mitochondrial function and metabolic maturation. Although a previous study has demonstrated the usefulness of engineered cardiac tissues to screen cardiotoxic compounds, the readout was based on the contraction of the cell construct [20], which might not be as sensitive as the metabolism component selected in this work. The impact of electric stimulation observed in cardiac cells cultured in MNF+PIEZO scaffolds is equivalent to results previously observed for CMs stimulated with external electric stimuli but using, in most cases, other biomarkers. Previous studies have shown that external electric current could trigger CM maturation, as demonstrated by shifts in gene expression profile [65-67], formation of extensive and organized myofibrils [65], increased levels of structural/contractile proteins [15], enlargement of CM cell body [65], enhanced intercellular coupling, better ultrastructural organization and alignment [15, 68]. Overall, the scaffold proposed here shows high potential to engineer cardiac tissue relevant for the *in vitro* screening of drugs.

3.6 Engineered human cardiac tissue in MNF+PIEZO scaffolds respond to compounds that modulate CM contraction. We then sought to investigate the response profile of the engineered human cardiac tissue to adrenergic receptor modulators (agonist: epinephrine; antagonist: propranolol) and blockers of intercellular communication (heptanol) (**Fig. 7A**). Therefore, cells cultured in MNF+PIEZO and PS for 12 days were loaded with a calcium-sensitive probe (Fluo-4), to monitor the mobilization of Ca^{2+} during cell contraction, and then

exposed to a specific pharmacologic agent. The concentrations tested were in the range reported by other studies to be non-cytotoxic [69-71]. Norepinephrine activates adrenergic receptors, which induces the permeability of Ca^{2+} channels at the cell membrane and sarcoplasmic reticulum, which in turn leads to an increase of intracellular Ca^{2+} concentration. Our results show that cardiac cells cultured in PS substrates have statistically lower beat frequency relatively to cells cultured in MNF+PIEZO, either in the absence or presence of norepinephrine (**Figs. 7B and 7C**).

Engineered human cardiac tissue in MNF+PIEZO scaffold was also evaluated in the presence of a β-blocker, propranolol. The high frequency of beatings induced by epinephrine was blocked by propanolol (2 μM) (**Fig. 7D**) but recovered after removing the media supplemented with propanolol with basal media (data not shown). We complemented these analyses by exposing the engineered human cardiac tissue to a cell-to-cell uncoupler, heptanol [69]. Low concentrations of heptanol (40 μM) reduced the propagation of action potential in the CMs analyzed (**Fig. 7E**) while high concentrations of heptanol (250 μM) completely blocked the beating of CMs. This effect that was reversed after the removal of the compound (data not shown).

Overall, our results show that cardiac cells cultured in MNF+PIEZO respond to contraction modulators, in the range of concentrations previously described for human CMs. In addition, in presence of norepinephrine, CMs cultured in MNF+PIEZO responded with higher number of beats than cells cultured in PS.

4. Conclusions

In conclusion, we have engineered a scaffold that combines several features to preserve CM contraction overtime and induce signs of cardiac maturation in cells of rat and human origin. The scaffold proposed in this work shows unique features (**Supplementary Table 2**). Firstly, the integration between a flexible polymeric matrix and anisotropically aligned piezoelectric fibers which induces cell alignment and converts mechanical stress, due to the CM contraction, in local electrical charges. Secondly, the whole system can be easily adapted for drug screening tests using cell metabolism as main readout. The properties of the engineered cardiac tissue have been compared to other engineered tissues containing inductive maturation elements (**Supplementary Table 3**). Although previous studies have used piezoelectric fibers with non-contractile cells [23, 72], few studies have explored the effect of piezoelectric materials in contractile cells such as cardiomyocytes [33, 73]. Indeed, the impact of piezoelectric polymers in human CM's function has not been previously documented. Our results indicate that MNF+PIEZO scaffold promotes cardiac cell attachment and alignment, maintains the ratio of cell populations (CFs:CMs) overtime, promotes cell-cell communication, and preserves CM contractility for at least 12 days. In addition, we have indications that MNF+PIEZO scaffold promotes CM maturation in two different cell models as shown by the increase in the expression of total Cx43 or phosphorylated Cx43, Ca^{2+} handling properties, expression of ion channels, metabolic profile, and response to cardiotoxic compounds that target mitochondria. Overall, the scaffold proposed here shows high potential to engineer cardiac tissue relevant for the *in vitro* screening of drugs. Future studies should further investigate the effect of piezoelectric materials in CM function. It is possible that the piezoelectric effect affects cardiomyocyte function/phenotype by interfering with cell membrane potential. In this case, transmembrane ion channels sensitive to voltage variations might be activated and opened, thus initiating a

process of depolarization of the cellular membrane and consequently cell contraction. It would be interesting to investigate the intracellular levels of Ca^{2+} in cells cultured in piezoelectric fibers by electrophysiology studies.

5. Acknowledgments

This work was supported by funds from FEDER through COMPETE program and Fundação para a Ciência e a Tecnologia (FCT) (EXPL/DTP-FTO/0570/2012, MITP-TB/ECE/0013/2013 to S. R. and L.F., and PTDC/SAU-ENB/113696/2009 to R.P.N.; SFRH/BD/51197/2010 and SFRH/BPD/79323/2011 to P.G. and S.R., respectively) as well as COMPETE program for the project "Stem cell based platforms for Regenerative and Therapeutic Medicine" (Centro-07-ST24-FEDER-002008). The authors also would like to acknowledge the help of Tommaso Mazzochi for the finite model simulations. The authors declare no conflict of interest to disclose.

6. References

[1] Eschenhagen T, Zimmermann WH. Engineering myocardial tissue. Circ Res. 2005;97:1220-31.
[2] Hirt MN, Hansen A, Eschenhagen T. Cardiac tissue engineering: state of the art. Circ Res. 2014;114:354-67.
[3] Vunjak-Novakovic G, Tandon N, Godier A, Maidhof R, Marsano A, Martens TP, et al. Challenges in Cardiac Tissue Engineering. Tissue Eng Part B-Re. 2010;16:169-87.
[4] Engelmayr GC, Jr., Cheng M, Bettinger CJ, Borenstein JT, Langer R, Freed LE. Accordion-like honeycombs for tissue engineering of cardiac anisotropy. Nat Mater. 2008;7:1003-10.
[5] Tian B, Liu J, Dvir T, Jin L, Tsui JH, Qing Q, et al. Macroporous nanowire nanoelectronic scaffolds for synthetic tissues. Nat Mater. 2012;11:986-94.
[6] Dvir T, Timko BP, Brigham MD, Naik SR, Karajanagi SS, Levy O, et al. Nanowired three-dimensional cardiac patches. Nat Nanotechnol. 2011;6:720-5.
[7] Wendel JS, Ye L, Tao R, Zhang J, Kamp TJ, Tranquillo RT. Functional Effects of a Tissue-Engineered Cardiac Patch From Human Induced Pluripotent Stem Cell-Derived Cardiomyocytes in a Rat Infarct Model. Stem Cells Transl Med. 2015;4:1324-32.
[8] Annabi N, Tsang K, Mithieux SM, Nikkhah M, Ameri A, Khademhosseini A, et al. Highly Elastic Micropatterned Hydrogel for Engineering Functional Cardiac Tissue. Adv Funct Mater. 2013;23.
[9] Thavandiran N, Dubois N, Mikryukov A, Masse S, Beca B, Simmons CA, et al. Design and formulation of functional pluripotent stem cell-derived cardiac microtissues. Proc Natl Acad Sci U S A. 2013;110:E4698-707.
[10] Aubin H, Nichol JW, Hutson CB, Bae H, Sieminski AL, Cropek DM, et al. Directed 3D cell alignment and elongation in microengineered hydrogels. Biomaterials. 2010;31:6941-51.
[11] Kim DH, Lipke EA, Kim P, Cheong R, Thompson S, Delannoy M, et al. Nanoscale cues regulate the structure and function of macroscopic cardiac tissue constructs. Proc Natl Acad Sci U S A. 2010;107:565-70.
[12] Chung C-Y, Bien H, Entcheva E. The Role of Cardiac Tissue Alignment in Modulating Electrical Function. Journal of Cardiovascular Electrophysiology. 2007;18:1323-9.
[13] You JO, Rafat M, Ye GJ, Auguste DT. Nanoengineering the heart: conductive scaffolds enhance connexin 43 expression. Nano Lett. 2011;11:3643-8.
[14] Nunes SS, Miklas JW, Liu J, Aschar-Sobbi R, Xiao Y, Zhang B, et al. Biowire: a platform for maturation of human pluripotent stem cell-derived cardiomyocytes. Nat Methods. 2013;10:781-7.
[15] Radisic M, Park H, Shing H, Consi T, Schoen FJ, Langer R, et al. Functional assembly of engineered myocardium by electrical stimulation of cardiac myocytes cultured on scaffolds. Proc Natl Acad Sci U S A. 2004;101:18129-34.
[16] Au HT, Cheng I, Chowdhury MF, Radisic M. Interactive effects of surface topography and pulsatile electrical field stimulation on orientation and elongation of fibroblasts and cardiomyocytes. Biomaterials. 2007;28:4277-93.
[17] Gwathmey JK, Tsaioun K, Hajjar RJ. Cardionomics: a new integrative approach for screening cardiotoxicity of drug candidates. Expert Opin Drug Metab Toxicol. 2009;5:647-60.
[18] Rodriguez B, Burrage K, Gavaghan D, Grau V, Kohl P, Noble D. The systems biology approach to drug development: application to toxicity assessment of cardiac drugs. Clin Pharmacol Ther. 2010;88:130-4.
[19] Mathur A, Loskill P, Shao K, Huebsch N, Hong S, Marcus SG, et al. Human iPSC-based cardiac microphysiological system for drug screening applications. Sci Rep. 2015;5:8883.

[20] Hansen A, Eder A, Bonstrup M, Flato M, Mewe M, Schaaf S, et al. Development of a drug screening platform based on engineered heart tissue. Circ Res. 2010;107:35-44.
[21] Baruscotti M, Barbuti A, Bucchi A. The cardiac pacemaker current. J Mol Cell Cardiol. 2010;48:55-64.
[22] Taccola S, Desii A, Pensabene V, Fujie T, Saito A, Takeoka S, et al. Free-Standing Poly(l-lactic acid) Nanofilms Loaded with Superparamagnetic Nanoparticles. Langmuir. 2011.
[23] Weber N, Lee YS, Shanmugasundaram S, Jaffe M, Arinzeh TL. Characterization and in vitro cytocompatibility of piezoelectric electrospun scaffolds. Acta Biomaterialia. 2010;6:3550-6.
[24] Boudaoud A, Burian A, Borowska-Wykret D, Uyttewaal M, Wrzalik R, Kwiatkowska D, et al. FibrilTool, an ImageJ plug-in to quantify fibrillar structures in raw microscopy images. Nat Protoc. 2014;9:457-63.
[25] Feinberg AW, Feigel A, Shevkoplyas SS, Sheehy S, Whitesides GM, Parker KK. Muscular Thin Films for Building Actuators and Powering Devices. Science. 2007;317:1366-70.
[26] Carisey A, Tsang R, Greiner AM, Nijenhuis N, Heath N, Nazgiewicz A, et al. Vinculin regulates the recruitment and release of core focal adhesion proteins in a force-dependent manner. Curr Biol. 2013;23:271-81.
[27] Lian X, Zhang J, Azarin SM, Zhu K, Hazeltine LB, Bao X, et al. Directed cardiomyocyte differentiation from human pluripotent stem cells by modulating Wnt/β-catenin signaling under fully defined conditions. Nature protocols. 2013;8:162-75.
[28] Lee H, Rho J, Messersmith PB. Facile Conjugation of Biomolecules onto Surfaces via Mussel Adhesive Protein Inspired Coatings. Adv Mater. 2009;21:431-4.
[29] Pereira GC, Pereira SP, Pereira CV, Lumini JA, Magalhaes J, Ascensao A, et al. Mitochondrionopathy phenotype in doxorubicin-treated Wistar rats depends on treatment protocol and is cardiac-specific. PLoS One. 2012;7:e38867.
[30] Liu X, Holzwarth JM, Ma PX. Functionalized synthetic biodegradable polymer scaffolds for tissue engineering. Macromol Biosci. 2012;12:911-9.
[31] Mandal D, Yoon S, Kim KJ. Origin of piezoelectricity in an electrospun poly(vinylidene fluoride-trifluoroethylene) nanofiber web-based nanogenerator and nano-pressure sensor. Macromol Rapid Commun. 2011;32:831-7.
[32] Weber N, Lee YS, Shanmugasundaram S, Jaffe M, Arinzeh TL. Characterization and in vitro cytocompatibility of piezoelectric electrospun scaffolds. Acta Biomater. 2010;6:3550-6.
[33] Hitscherich P, Wu S, Gordan R, Xie LH, Arinzeh T, Lee EJ. The effect of PVDF-TrFE scaffolds on stem cell derived cardiovascular cells. Biotechnol Bioeng. 2016;113:1577-85.
[34] Kholkin A, Amdursky N, Bdikin I, Gazit E, Rosenman G. Strong piezoelectricity in bioinspired peptide nanotubes. ACS Nano. 2010;4:610-4.
[35] Yasuda N, Banno T, Fujita K, Ohwa H, Matushita M, Yamashita Y, et al. Pressure dependence of piezoelectric properties of a Pb(Mg(1/3)Nb(2/3))O(3)-PbTiO(3) binary system single crystal near a morphotropic phase boundary. J Phys Condens Matter. 2006;18:7659-68.
[36] Leor J, Aboulafia-Etzion S, Dar A, Shapiro L, Barbash IM, Battler A, et al. Bioengineered cardiac grafts: A new approach to repair the infarcted myocardium? Circulation. 2000;102:Iii56-61.
[37] Baumgartner S, Halbach M, Krausgrill B, Maass M, Srinivasan SP, Sahito RG, et al. Electrophysiological and morphological maturation of murine fetal cardiomyocytes during electrical stimulation in vitro. J Cardiovasc Pharmacol Ther. 2015;20:104-12.
[38] Yang X, Pabon L, Murry CE. Engineering adolescence: maturation of human pluripotent stem cell-derived cardiomyocytes. Circ Res. 2014;114:511-23.

[39] Tiburcy M, Didie M, Boy O, Christalla P, Doker S, Naito H, et al. Terminal differentiation, advanced organotypic maturation, and modeling of hypertrophic growth in engineered heart tissue. Circ Res. 2011;109:1105-14.
[40] Radisic M, Park H, Martens TP, Salazar-Lazaro JE, Geng W, Wang Y, et al. Pre-treatment of synthetic elastomeric scaffolds by cardiac fibroblasts improves engineered heart tissue. J Biomed Mater Res A. 2008;86:713-24.
[41] Biela SA, Su Y, Spatz JP, Kemkemer R. Different sensitivity of human endothelial cells, smooth muscle cells and fibroblasts to topography in the nano-micro range. Acta Biomater. 2009;5:2460-6.
[42] Discher DE, Janmey P, Wang YL. Tissue cells feel and respond to the stiffness of their substrate. Science. 2005;310:1139-43.
[43] Fujie T, Ahadian S, Liu H, Chang H, Ostrovidov S, Wu H, et al. Engineered nanomembranes for directing cellular organization toward flexible biodevices. Nano Lett. 2013;13:3185-92.
[44] Shi XT, Fujie T, Saito A, Takeoka S, Hou Y, Shu YW, et al. Periosteum-Mimetic Structures Made from Freestanding Microgrooved Nanosheets. Advanced Materials. 2014;26:3290-+.
[45] Ricotti L, Polini A, Genchi GG, Ciofani G, Iandolo D, Vazao H, et al. Proliferation and skeletal myotube formation capability of C2C12 and H9c2 cells on isotropic and anisotropic electrospun nanofibrous PHB scaffolds. Biomed Mater. 2012;7:035010.
[46] Akhilesh KG, Mehdi N, Shilpa S, Ali K. Anisotropic poly (glycerol sebacate)-poly (ϵ -caprolactone) electrospun fibers promote endothelial cell guidance. Biofabrication. 2015;7:015001.
[47] Marquez-Rosado L, Solan JL, Dunn CA, Norris RP, Lampe PD. Connexin43 phosphorylation in brain, cardiac, endothelial and epithelial tissues. Biochim Biophys Acta. 2012;1818:1985-92.
[48] Zhang D, Shadrin IY, Lam J, Xian HQ, Snodgrass HR, Bursac N. Tissue-engineered cardiac patch for advanced functional maturation of human ESC-derived cardiomyocytes. Biomaterials. 2013;34:5813-20.
[49] Ando M, Katare RG, Kakinuma Y, Zhang D, Yamasaki F, Muramoto K, et al. Efferent vagal nerve stimulation protects heart against ischemia-induced arrhythmias by preserving connexin43 protein. Circulation. 2005;112:164-70.
[50] Radisic M, Christman KL. Materials science and tissue engineering: repairing the heart. Mayo Clin Proc. 2013;88:884-98.
[51] Loe MJ, Edwards WD. A light-hearted look at a lion-hearted organ (or, a perspective from three standard deviations beyond the norm). Part 1 (of two parts). Cardiovasc Pathol. 2004;13:282-92.
[52] Xia Y, McMillin JB, Lewis A, Moore M, Zhu WG, Williams RS, et al. Electrical Stimulation of Neonatal Cardiac Myocytes Activates the NFAT3 and GATA4 Pathways and Up-regulates the Adenylosuccinate Synthetase 1 Gene. Journal of Biological Chemistry. 2000;275:1855-63.
[53] Shin SR, Jung SM, Zalabany M, Kim K, Zorlutuna P, Kim SB, et al. Carbon-nanotube-embedded hydrogel sheets for engineering cardiac constructs and bioactuators. ACS Nano. 2013;7:2369-80.
[54] Khademhosseini A, Eng G, Yeh J, Kucharczyk PA, Langer R, Vunjak-Novakovic G, et al. Microfluidic patterning for fabrication of contractile cardiac organoids. Biomed Microdevices. 2007;9:149-57.
[55] Radisic M, Yang L, Boublik J, Cohen RJ, Langer R, Freed LE, et al. Medium perfusion enables engineering of compact and contractile cardiac tissue. Am J Physiol Heart Circ Physiol. 2004;286:H507-16.

[56] VanPutte C, Regan J, Russo A. Seeley's Essentials of Anatomy and Physiology: McGraw-Hill Science/Engineering/Math; 2015.
[57] Correia C, Koshkin A, Carido M, Espinha N, Saric T, Lima PA, et al. Effective Hypothermic Storage of Human Pluripotent Stem Cell-Derived Cardiomyocytes Compatible With Global Distribution of Cells for Clinical Applications and Toxicology Testing. Stem Cells Transl Med. 2016;5:658-69.
[58] Bergmann O, Zdunek S, Felker A, Salehpour M, Alkass K, Bernard S, et al. Dynamics of Cell Generation and Turnover in the Human Heart. Cell. 2015;161:1566-75.
[59] Howard CM, Baudino TA. Dynamic cell–cell and cell–ECM interactions in the heart. Journal of Molecular and Cellular Cardiology. 2014;70:19-26.
[60] Kléber AG, Rudy Y. Basic Mechanisms of Cardiac Impulse Propagation and Associated Arrhythmias. Physiological Reviews. 2004;84:431-88.
[61] Lopaschuk GD, Jaswal JS. Energy metabolic phenotype of the cardiomyocyte during development, differentiation, and postnatal maturation. J Cardiovasc Pharmacol. 2010;56:130-40.
[62] Octavia Y, Tocchetti CG, Gabrielson KL, Janssens S, Crijns HJ, Moens AL. Doxorubicin-induced cardiomyopathy: from molecular mechanisms to therapeutic strategies. J Mol Cell Cardiol. 2012;52:1213-25.
[63] Ichikawa Y, Ghanefar M, Bayeva M, Wu R, Khechaduri A, Prasad SVN, et al. Cardiotoxicity of doxorubicin is mediated through mitochondrial iron accumulation. The Journal of Clinical Investigation. 2014;124:617-30.
[64] Frost BM, Eksborg S, Bjork O, Abrahamsson J, Behrendtz M, Castor A, et al. Pharmacokinetics of doxorubicin in children with acute lymphoblastic leukemia: multi-institutional collaborative study. Med Pediatr Oncol. 2002;38:329-37.
[65] McDonough PM, Glembotski CC. Induction of atrial natriuretic factor and myosin light chain-2 gene expression in cultured ventricular myocytes by electrical stimulation of contraction. Journal of Biological Chemistry. 1992;267:11665-8.
[66] Xia Y, Buja LM, McMillin JB. Activation of the Cytochrome c Gene by Electrical Stimulation in Neonatal Rat Cardiac Myocytes: ROLE OF NRF-1 AND c-Jun. Journal of Biological Chemistry. 1998;273:12593-8.
[67] Passier R, Zeng H, Frey N, Naya FJ, Nicol RL, McKinsey TA, et al. CaM kinase signaling induces cardiac hypertrophy and activates the MEF2 transcription factor in vivo. Journal of Clinical Investigation. 2000;105:1395-406.
[68] Tandon N, Cannizzaro C, Chao PH, Maidhof R, Marsano A, Au HT, et al. Electrical stimulation systems for cardiac tissue engineering. Nat Protoc. 2009;4:155-73.
[69] Caspi O, Itzhaki I, Kehat I, Gepstein A, Arbel G, Huber I, et al. In Vitro Electrophysiological Drug Testing Using Human Embryonic Stem Cell Derived Cardiomyocytes. Stem Cells Dev. 2009;18:161-72.
[70] Lan F, Lee AS, Liang P, Sanchez-Freire V, Nguyen PK, Wang L, et al. Abnormal calcium handling properties underlie familial hypertrophic cardiomyopathy pathology in patient-specific induced pluripotent stem cells. Cell Stem Cell. 2013;12:101-13.
[71] Maddah M, Heidmann JD, Mandegar MA, Walker CD, Bolouki S, Conklin BR, et al. A non-invasive platform for functional characterization of stem-cell-derived cardiomyocytes with applications in cardiotoxicity testing. Stem Cell Reports. 2015;4:621-31.
[72] Lee Y-S, Collins G, Livingston Arinzeh T. Neurite extension of primary neurons on electrospun piezoelectric scaffolds. Acta Biomaterialia. 2011;7:3877-86.
[73] Liu X, Zhao H, Lu Y, Li S, Lin L, Du Y, et al. In vitro cardiomyocyte-driven biogenerator based on aligned piezoelectric nanofibers. Nanoscale. 2016;8:7278-86.

Main Figures & Supplementary Figures

Flexible nanofilms coated with aligned piezoelectric microfibers preserve the long-term contractility of cardiomyocytes

*P. José Gouveia #, ##, S. Rosa #, L. Ricotti §, B. Abecasis § §, H. V. Almeida #, L. Monteiro #, J. Nunes ‡, F. Sofia Carvalho #, ##, M. Serra § §, S. Luchkin ††, A. Leonidovitch Kholkin ††, P.Marques Alves § § , P. Jorge Oliveira ##, R. Carvalho ##†, A. Menciassi §, R. Pires Neves #, L. Silva Ferreira * #*

 # CNC-Center of Neurosciences and Cell Biology, University of Coimbra; 3004-517 Coimbra, Portugal
Instituto de Investigação Interdisciplinar, University of Coimbra, Casa Costa Alemão - Pólo II, Rua Dom Francisco de Lemos, 3030-789, Coimbra, Portugal.
§ The BioRobotics Institute, Scuola Superiore Sant' Anna, Viale Rinaldo Piaggio 34, 56025 Pontedera (PI), Italy
§ § Inst. de Tecnologia Química e Biologica António Xavier, New University of Lisbon, Av. da Republica, 2780-157 Oeiras, Portugal
† Department of Life Sciences, Faculty of Sciences and Technology, University of Coimbra, 3000-456 Coimbra, Portugal
†† CICECO - Materials Institute of Aveiro & Physics Dept, University of Aveiro, Campus de Santiago, 3810-193 Aveiro, Portugal.
‡ Centre for Mechanical Engineering, University of Coimbra, Coimbra, Portugal;
3030-788 Coimbra, Portugal
** Corresponding author (Email:Lino@biocant.pt)*

KEYWORDS: cardiac tissue engineering, nanofilms, electrospun fibers, piezoelectric materials, cardiotoxicity

[*] Corresponding author: Lino S. Ferreira

Keywords: cardiac tissue engineering, nanofilms, electrospun fibers, piezoelectric materials, cardiotoxicity

Figure 1

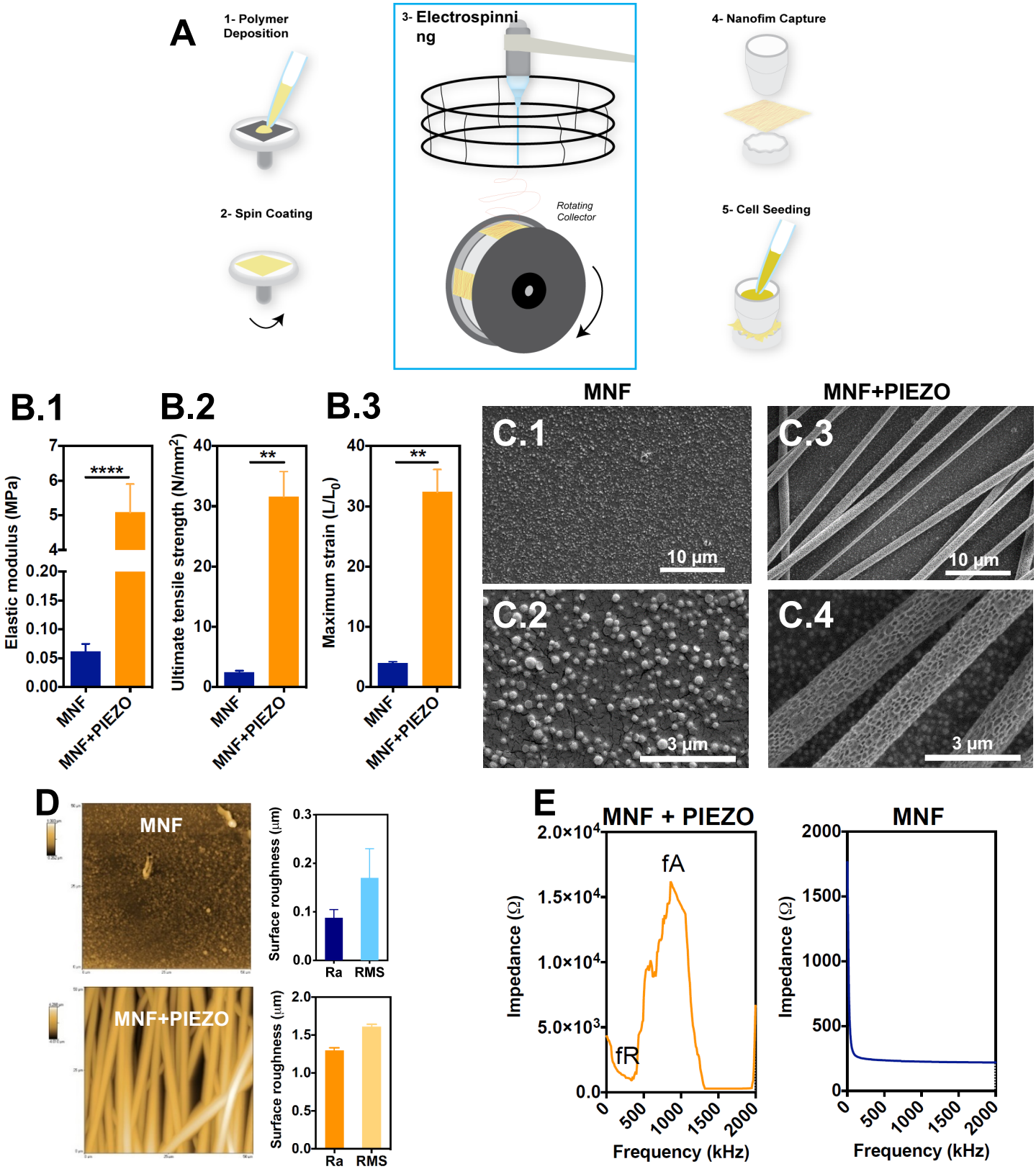

Figure 1 - Preparation and characterization of MNF and MNF+PIEZO scaffolds. (A) Scheme showing the methodology used for the preparation of MNF and MNF+PIEZO. Initially, a sacrificial layer of poly(vinyl alcohol) was deposited in a silicon wafer and spin-coated. This was followed by the spin-coating of a solution of PCL, deposition of PIEZO fibers by electrospinning, mounting the scaffold in a cell crown system and culture the cells on top of it. **(B)** Mechanical properties of MNF and MNF+PIEZO scaffolds obtained by stress-strain measurements, including elastic modulus (B.1), maximum strain (B.2) and ultimate tensile strength (B.3). The nanofilms were immersed in water to remove them from the silicon substrate and allow their fixation into the mechanical testing system. Results are Average ± SEM, n=10. **(C)** Scanning electron microscopy (SEM) images of the surface of MNF (C.1 and C.2) and MNF+PIEZO (C.3 and C.4). **(D)** Atomic force microscopy (AFM) images of MNF and MNF+PIEZO (tapping mode; height imaging). Scan areas of 50×50 mm^2 were used. Graphs show roughness average (Ra) and root mean square (RMS) roughness. Results are Average ± SEM, n=4. **(E)** Impedance spectra of MNF and MNF+PIEZO scaffolds. The MNF+PIEZO spectrum has two characteristic frequencies (resonance frequency, f_R, and anti-resonance frequency, f_A), typically of piezoelectric materials. The MNF spectrum shows no characteristic peaks in the frequency interval tested.

Figure 2

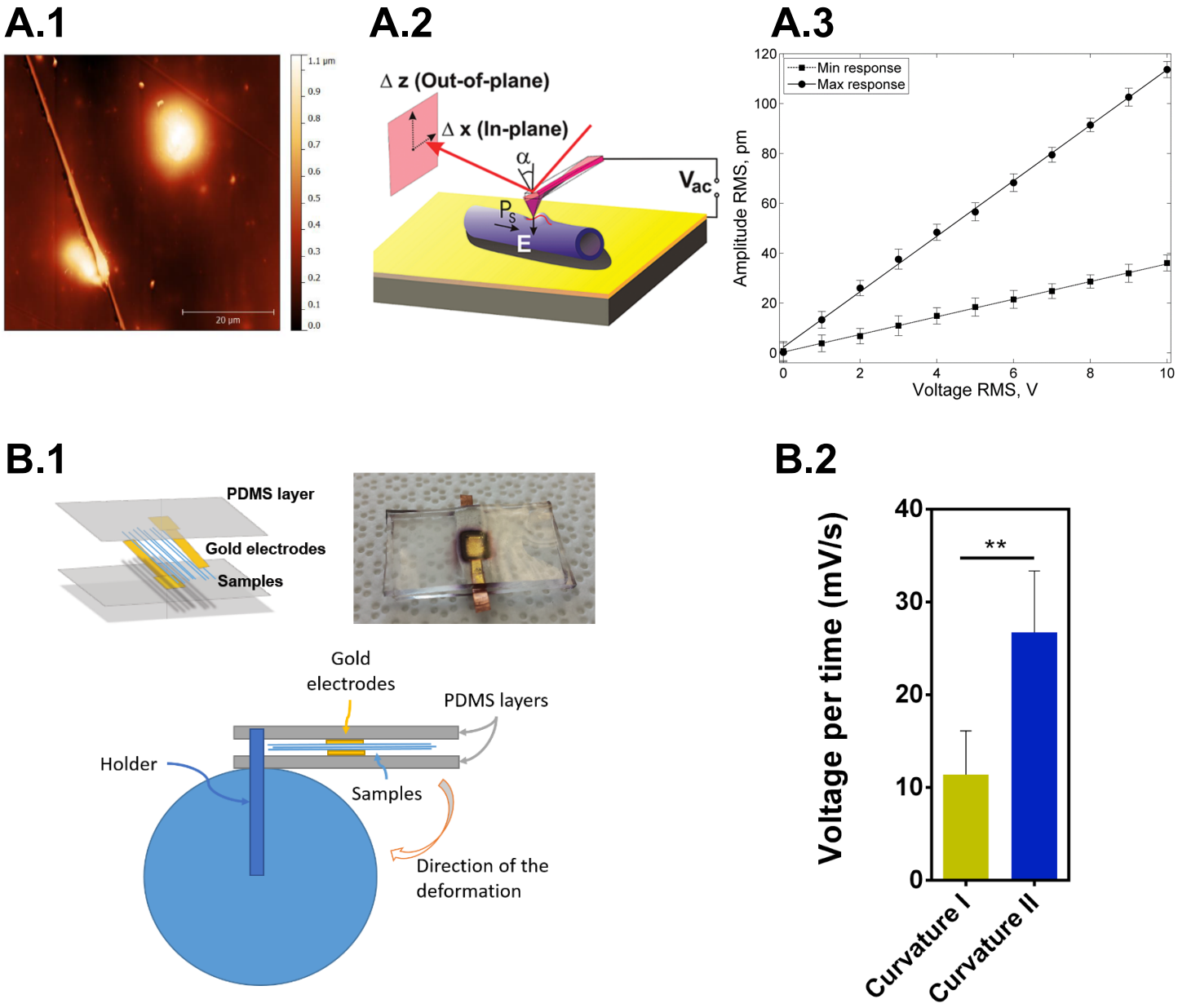

Figure 2 - Piezoelectric properties of PIEZO fibers and MNF + PIEZO scaffolds. (A) Assessment of piezoelectric properties of PIEZO microfibers by PMF. (A.1) AFM images of the PIEZO microfibers. (A.2) Procedure for the determination of piezoelectric properties. (A.3) Amplitude of displacement as a function of AC voltage applied to the samples. The determined piezoelectric charge constant, d, refers to the induced strain in direction 3 per unit electric field applied in direction 3 (d_{33}). Results are Average ± SEM, n=5. **(B)** Methodology for the assessment of the piezoelectric properties in the PIEZO microfibers (B.1). Assessment of the direct piezoelectric effect in PIEZO microfibers (B.2). PIEZO microfibers were submitted to mechanical deformations at two different curvature values (curvature I refers to the substrate deformed over the external surface of a Delrin cylinder showing a diameter of 84 mm; curvature II refers to the substrate deformed over the external surface of a Delrin cylinder showing a diameter of 105 mm), while registering the amount of voltage generated over time (values normalized towards control; Average= 0.00263 mV/s). Results are Average ± SEM, n=10. * Denotes statistical significance: **P<0.01.

Figure 3

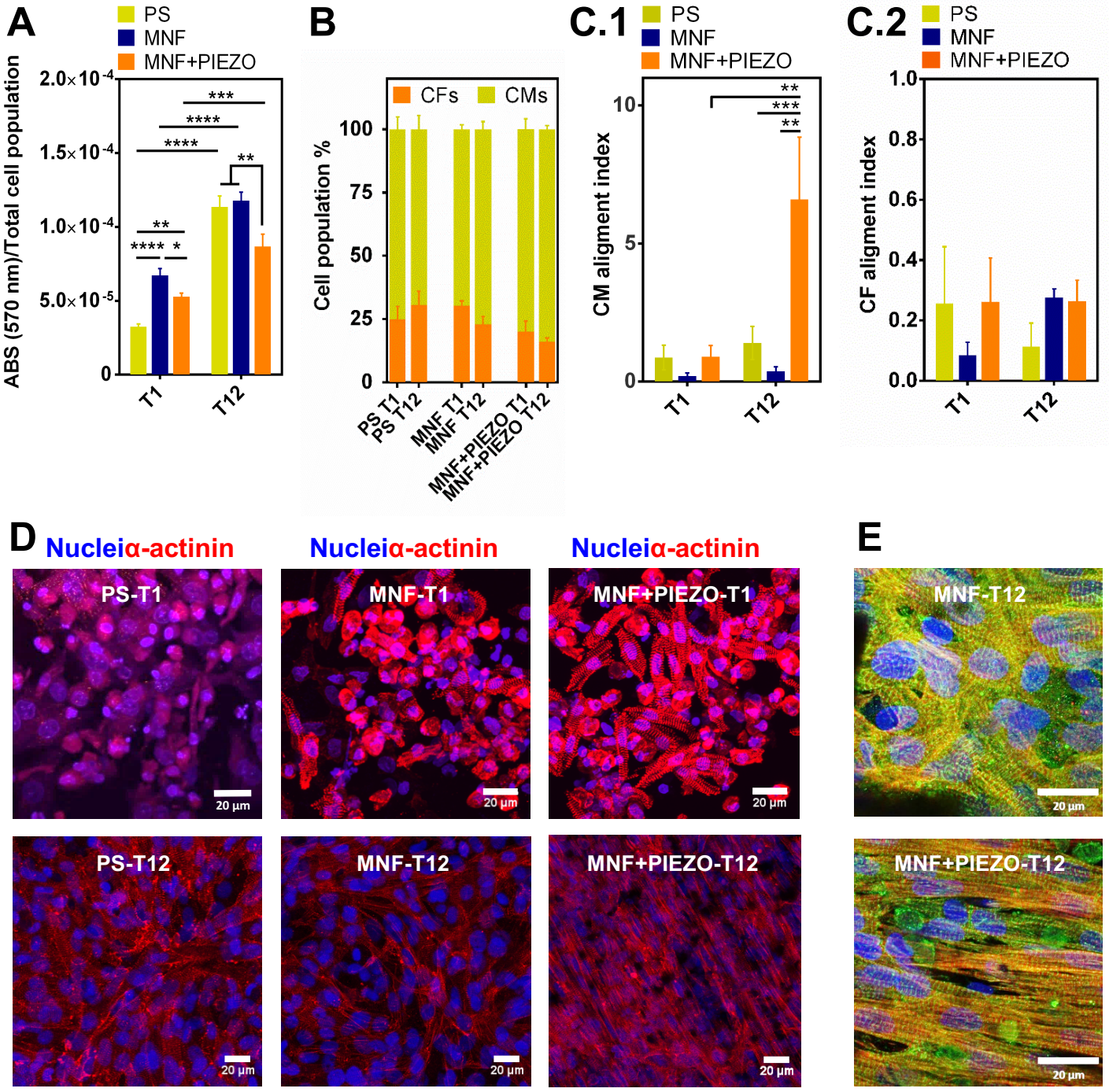

Figure 3 - Viability, composition and alignment of rat prenatal cardiac cells cultured in different scaffolds. (A) Cell viability/proliferation as assessed by a MTT assay. Results are Average ± SEM, n=6. **(B)** Quantification of CM and CF total population per culture area (0.8 cm^2) done by confocal microscopy with in immunostained samples (objective 63×). Results are Average ± SEM, n=3 (three independent experiments; each experiment having at least 3 technical replicas). **(C)** CM and CF sub-population alignment index in different substrates. The alignment was calculated through confocal microscopy images (63×) of immunostained samples. CM and CF sub-population alignment index in different substrates. The alignment was calculated in confocal microscopy images (63×) of immunostained samples. Cellular alignment was quantified by taking account the deviation (20º degrees) towards a common reference line. CM population was identified as positive for α-actinin staining while CF population was identified as positive for vimentin. Results are Average ± SEM, n=3 (three independent experiments; each experiment having at least 3 technical replicas). **(D)** Representative confocal microscopy images of cardiac cells cultured in the different substrates tested for 1 day (T1) and 12 days after seeding (T12). Cells were stained for sarcomeric α-actinin. Scale bar represents 20 µm. **(E)** Representative confocal images of positive sarcomeric α-actinin and troponin I CMs cultured under different substrates at T1 and T12. In A and C.1, * denotes statistical significance: *P<0.05, **P<0.01, ***P<0.001, ****P<0.0001.

Figure 4

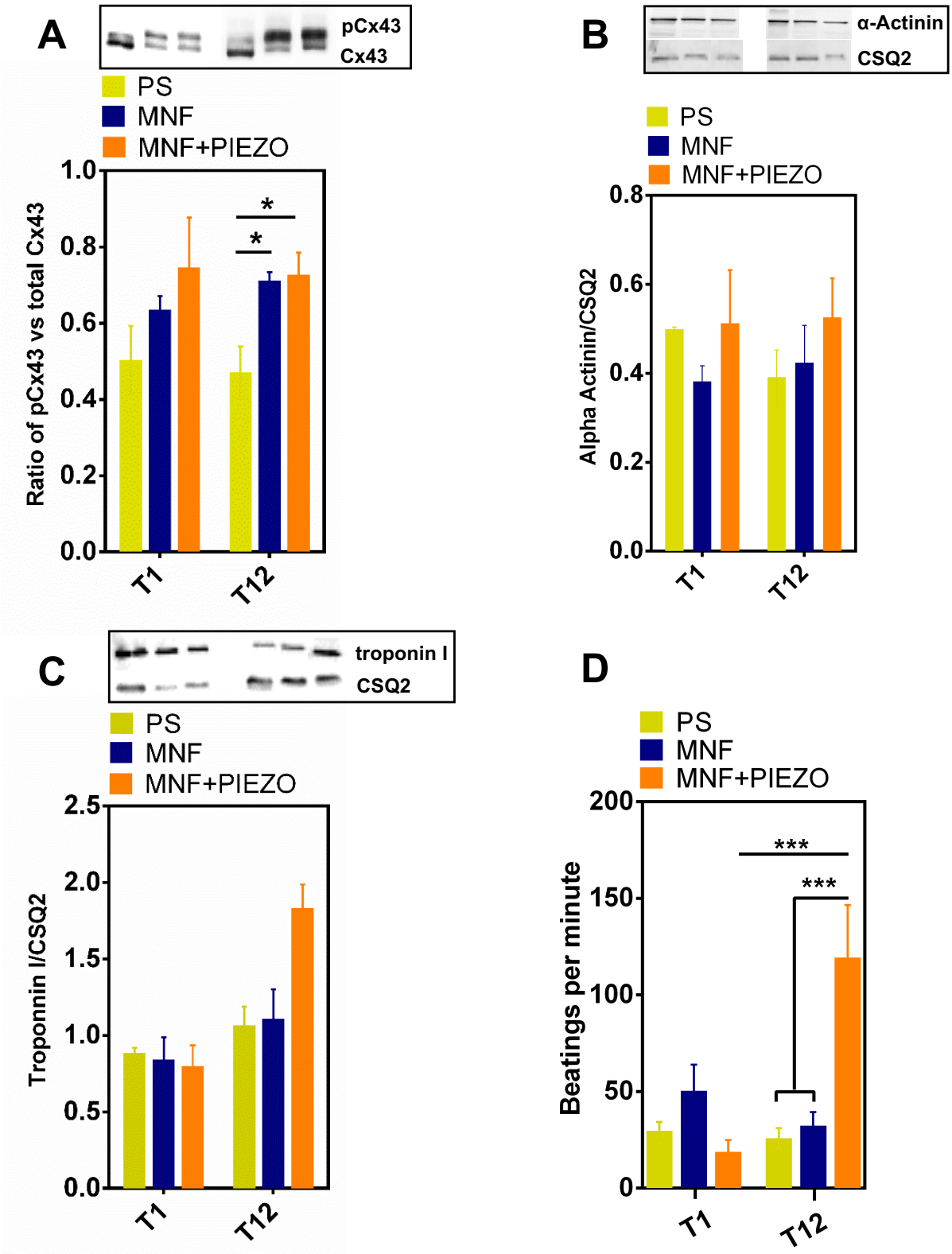

Figure 4 - Contraction and expression of sarcomeric (a-actinin, troponin I) and gap junction connexin 43 proteins of rat prenatal cardiac cells cultured in different scaffolds. (A) Ratio of phosphorylated versus total connexin 43, at day 1 and 12 of culture (n = 3, 3 replicas at minimum). **(B)** Sarcomeric α-actinin expression at 1 and 12 days of culture (n = 3, 3 replicas at minimum) normalized to the expression of calsequestrin 2 (CSQ2). **(C)** Troponin I protein levels at T1 and T12 (n = 3, 3 replicas at minimum) normalized to the expression of CSQ2. **(D)** Average of spontaneous cardiac tissue beatings per minute (average of 7 independent experiments n = 7, 3 replicates at minimum per experiment). In A, B and C, representative western blots are shown on top of the graph. In A, B, C and D, results are Average ± SEM. * Denotes statistical significance: *P<0.05, **P<0.01, ***P<0.001, ****P<0.0001

Figure 5

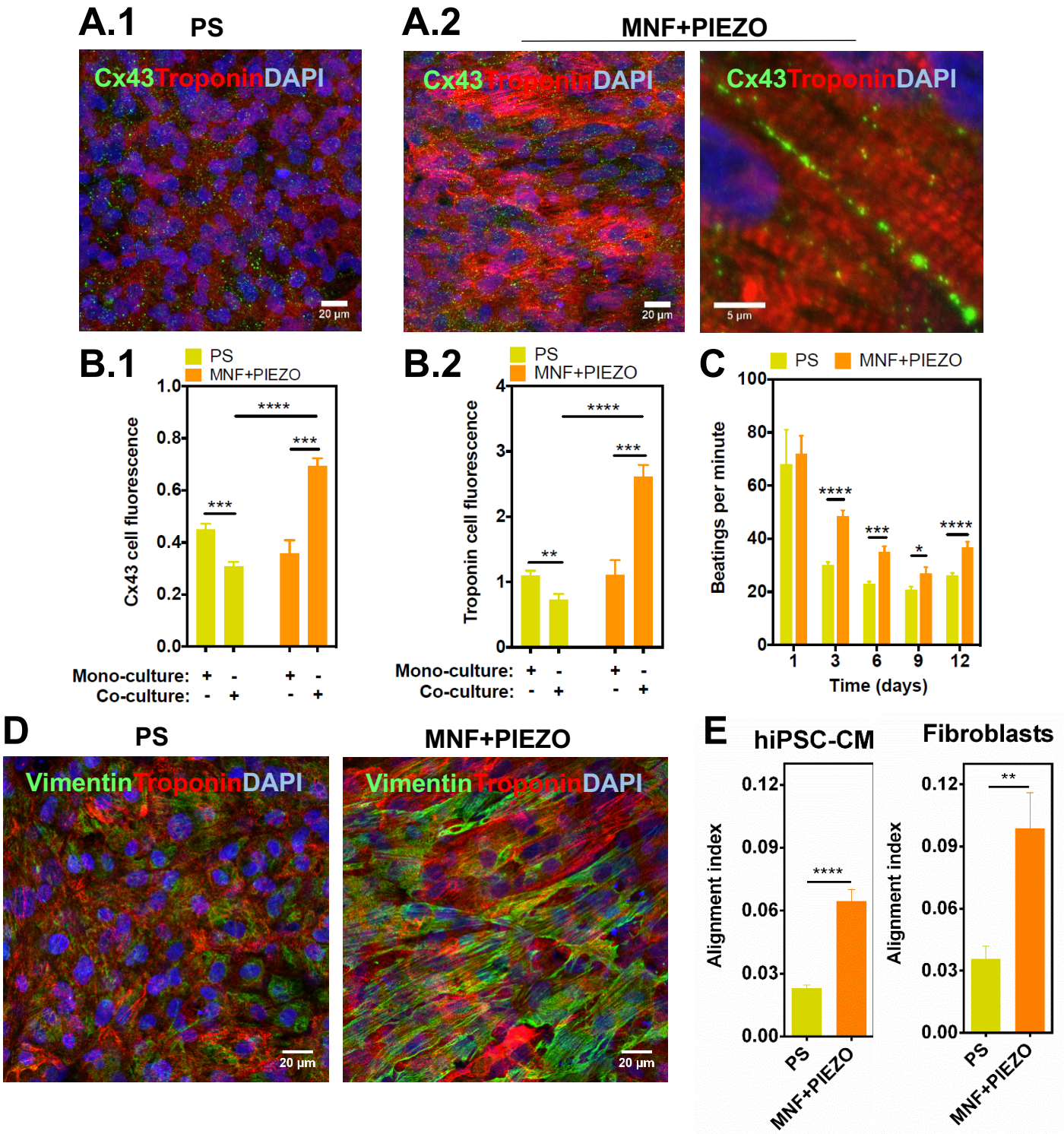

Figure 5 - Expression of Cx43 and proteins of contractile machinery in human cells at day 12. (A) Confocal microscope images of human cardiac cells cultured in PS (A.1) or MNF+PIEZO (A.2) for 12 days. Images show the expression and localisation of total Cx43 and Troponin (sub-units I and T) in a co-culture of hiPSC-CM with fibroblasts. Scale bar represents 20 µm and 5 µm for the low and high magnification images, respectively. **(B)** Quantification of cell fluorescence for total Cx43 and Troponin from confocal microscope images. Results are Average ± SEM (n=2, 4 technical replicates for each n). **(C)** Average of spontaneous beatings per minute in CMs co-cultured with fibroblasts in PS or MNF+PIEZO scaffold. Average ± SEM (n=1, 11 replicates for each n). **(D)** Representative confocal microscopy images of co-culture of hiPSC-CM with fibroblasts on PS or MNF+PIEZO scaffold. Scale bar represents 20 µm. **(E)** Alignment index for hiPSC-CMs and fibroblasts cultured in PS or MNF +PIEZO scaffolds. The alignment was calculated in immuno-stained samples (CMs stained for troponin T; fibroblasts stained for vimentin). Cellular alignment was quantified by using ImageJ's plugin FibrilTool. In B, C and E, * denotes statistical significance: *P<0.05, **P<0.01, ***P<0.001, ****P<0.0001.

Figure 6

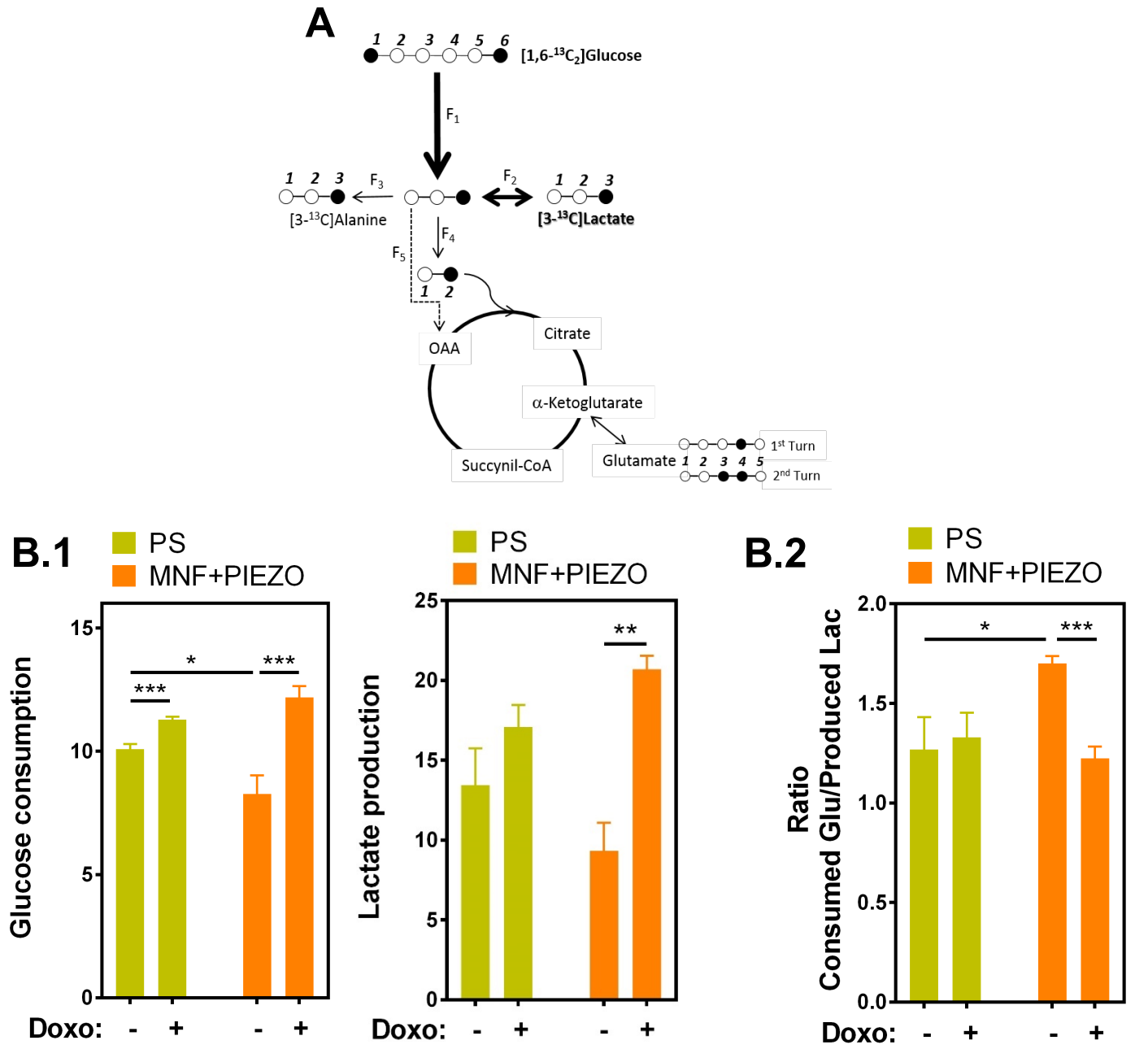

Figure 6 - Effect of DOXO in the metabolism of human cardiac cells cultured in MNF+PIEZO scaffolds. (A) Cellular metabolism was evaluated using the carbon tracer [1,6-13C2]glucose and proton nuclear magnetic resonance spectroscopy (1H-NMR). Schematic representation of the metabolic fluxes: F1-glucose consumption; F2-lactic acid fermentation; F3-pyruvate transamination; F4-pyruvate oxidation; F5-pyruvate carboxylation. Through glycolysis, [1,6-13C2]glucose gets converted into two molecules of [3-13C]pyruvate, that can follow any of the previously mentioned pathways/fates. **(B)** Human cardiac cells were cultured for 12 days in MNF+PIEZO scaffolds before exposure to DOXO. Cell metabolism was monitored by NMR. **(B.1)** Rates of glucose consumption and lactate production in the presence (+) and absence (-) of DOXO. **(B.2)** Ratio of glucose consumption and lactate production. High ratio´s means high oxidative phosphorylation. DOXO treatment causes significant increase in glucose consumption in both PS and MNF+PIEZO groups and promotes an increase in lactate production only in the MNF+PIEZO group. These results suggest that cardiac cells in the PS group are more glycolytic than in the MNF+PIEZO. In B, results are Average ± SEM, n=2 (two independent experiments; each experiment having at least 3 technical replicates). *Denotes statistical significance: *P<0.05, **P<0.01, ***P<0.001 (unpaired t-test between experimental groups).

Figure 7

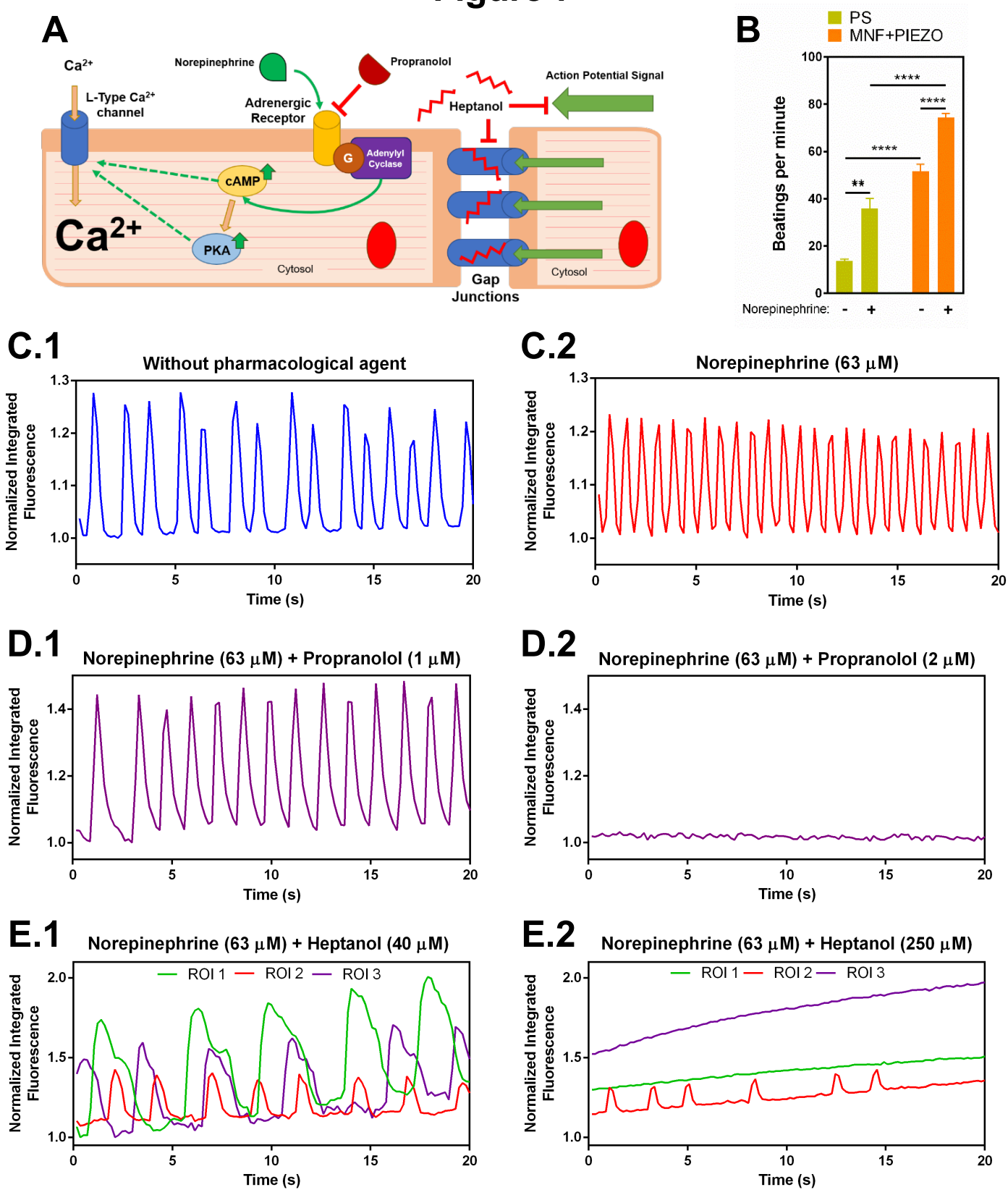

Figure 7 - Live cell imaging of intracellular Ca^{2+}. A co-culture of hiPSC-CMs with fibroblasts was cultured in MNF+PIEZO scaffolds (for one condition the cells were also cultured in PS substrate) for 12 days before analysis. Intracellular calcium levels as monitored by using the Fluo-4 Ca^{2+} sensitive probe. **(A)** Scheme showing the pharmacological action of the drugs tested. **(B)** Effect of norepinephrine (63 µM) in the beating frequency of CMs cultured for 12 days in PS or MNF+PIEZO scaffolds. Results are ± SEM, n=1 (4-12 ROIs were used from a representative video recording for the quantifications). *Denotes statistical significance: **P<0.01, ***P<0.001, ****P<0.0001, (unpaired t-test between experimental groups). **(C)** Representative traces of intracellular Ca^{2+} in CMs cultured without drugs (C.1) or with norepinephrine (C.2). **(D)** Representative traces of intracellular Ca^{2+} in CMs cultured with norepinephrine in the presence of increasing concentrations of β-blocker, propranolol. In C and D, Ca^{2+} profiles are the average of 3 ROIs from a representative video recording. **(E)** Representative traces of intracellular Ca^{2+} in CMs cultured with norepinephrine in the presence of gap junction uncoupler heptanol. Each intracellular Ca^{2+} trace corresponds to a single ROI obtained from a representative video recording. The three traces indicate an asynchronous beating rate of CMs in which gap junctions have been disrupted by heptanol.

Supplementary Figure 1

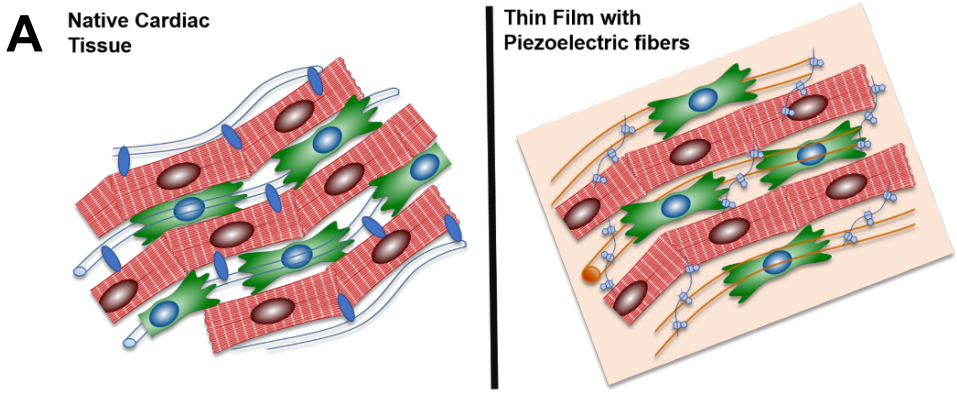

Aligned Type 1/3 collagen fibers (100 nm)	**Topography**	Aligned piezoelectric microfibers (1 µm)
Collagen, fibronectin, laminin	**ECM composition**	Gelatin
25 kPa	**Mechanical properties**	5 MPa
Cell based electrochemical signalling	**Electrical properties**	Electric charge generation upon deformation
Cardiomyocytes and Cardiac Fibroblasts	**Main Cell Types**	Cardiomyocytes and Cardiac Fibroblasts

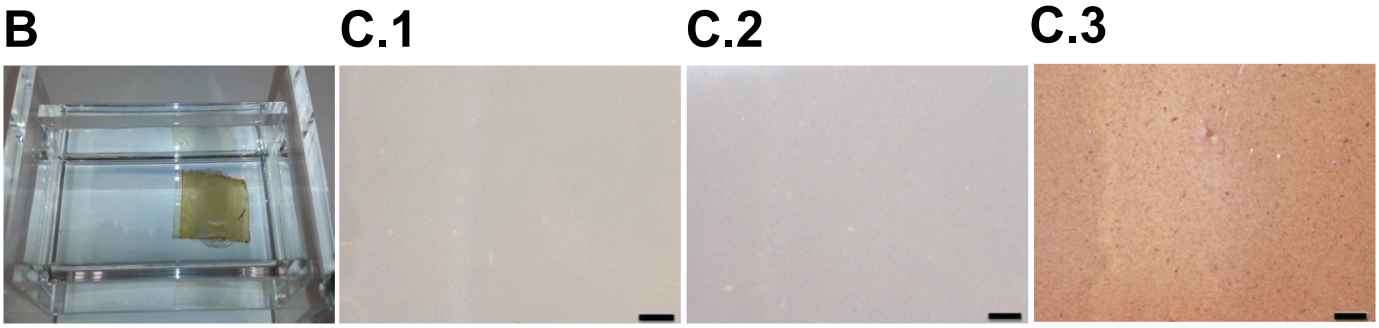

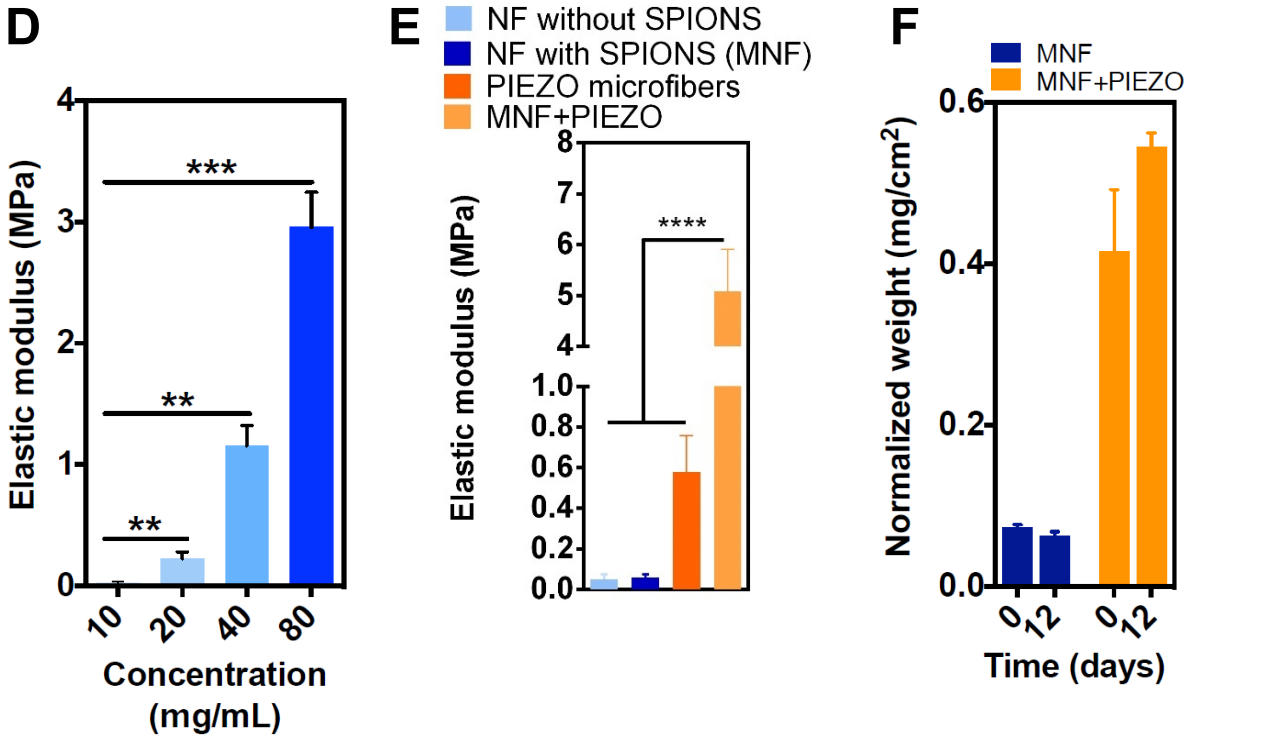

Supplementary Fig. 1 - Morphology and mechanical properties of the nanofilms. (A) Properties of native cardiac tissue and engineered cardiac tissue. The engineered cardiac tissue is a compromise between technical feasibility to integrate all aspects of the cardiac ECM and the actual native cardiac properties. **(B)** Nanofilm removed from the silicon wafer and immersed in water. **(C)** Morphology of the nanofilms prepared with different concentrations of PCL (C.1: 20 mg/mL; C.2: 40 mg/mL; C.3: 80 mg/mL) as evaluated by light microscopy. Bar corresponds to 500 µm. **(D)** Elastic modulus of nanofilms prepared with different concentrations of PCL. Results are Average ± SEM, n=3-5. **(E)** Elastic modulus for nanofilms with (MNF) and without SPIONs and MNF with (MNF+PIEZO) and without PIEZO microfibers. **(F)** Degradation studies of MNF and MNF+PIEZO in the presence of a solution of trypsin and collagenase type II (20 ng/mL for trypsin and 350 µg/mL for collagenase, both in PBS; these enzyme concentrations have been used for heart tissue digestion) for 12 days at 37ºC. Results are Average ± SEM, n=3-5. In D and E, * denotes statistical significance: *P<0.05, **P<0.01, ***P<0.001, ****P<0.0001.

Supplementary Figure 2

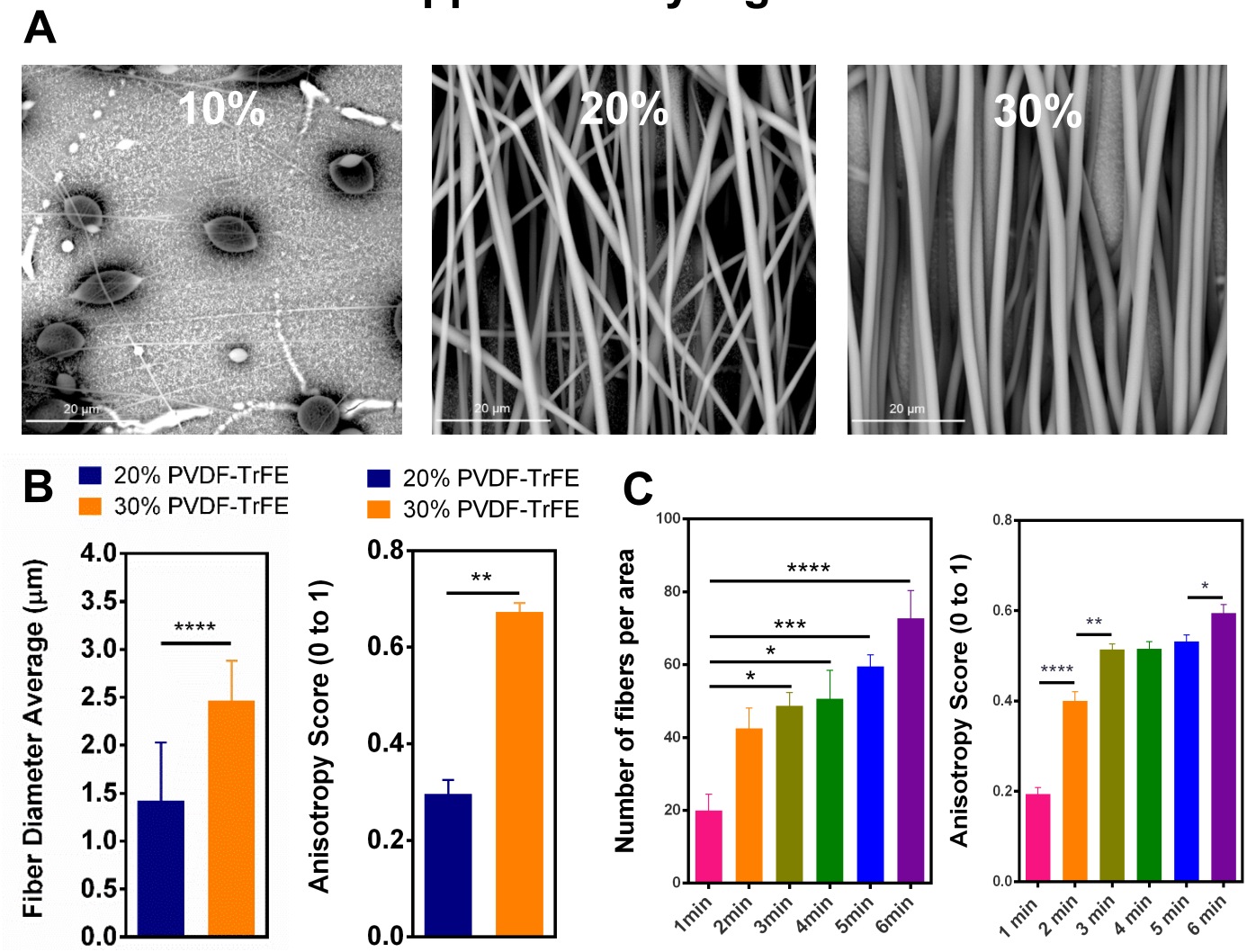

Supplementary Fig. 2 - Morphology, diameter and anisotropy of the PIEZO fibers. (**A**) SEM images of the PIEZO fibers deposited on top of the PCL nanofilm. Concentrations of PVDF-TrFE (%, w/v) are indicated on top of the images. Bar corresponds to 20 µm. (**B**) Diameter (n>950 fibers) and anisotropy (n=4) of fibers prepared from a solution of 20 and 30 % (w/v) of PVDF-TrFE. Results are Average ± SEM. Anisotropy of 1 indicates that fibers are not aligned. (**C**) Number of fibers per area and anisotropy score of the fibers as a function of deposition time on top of the nanofilm. Results are Average ± SEM, n=4. In B and C, * denotes statistical significance: *P<0.05, **P<0.01, ***P<0.001, ****P<0.0001.

Supplementary Figure 3

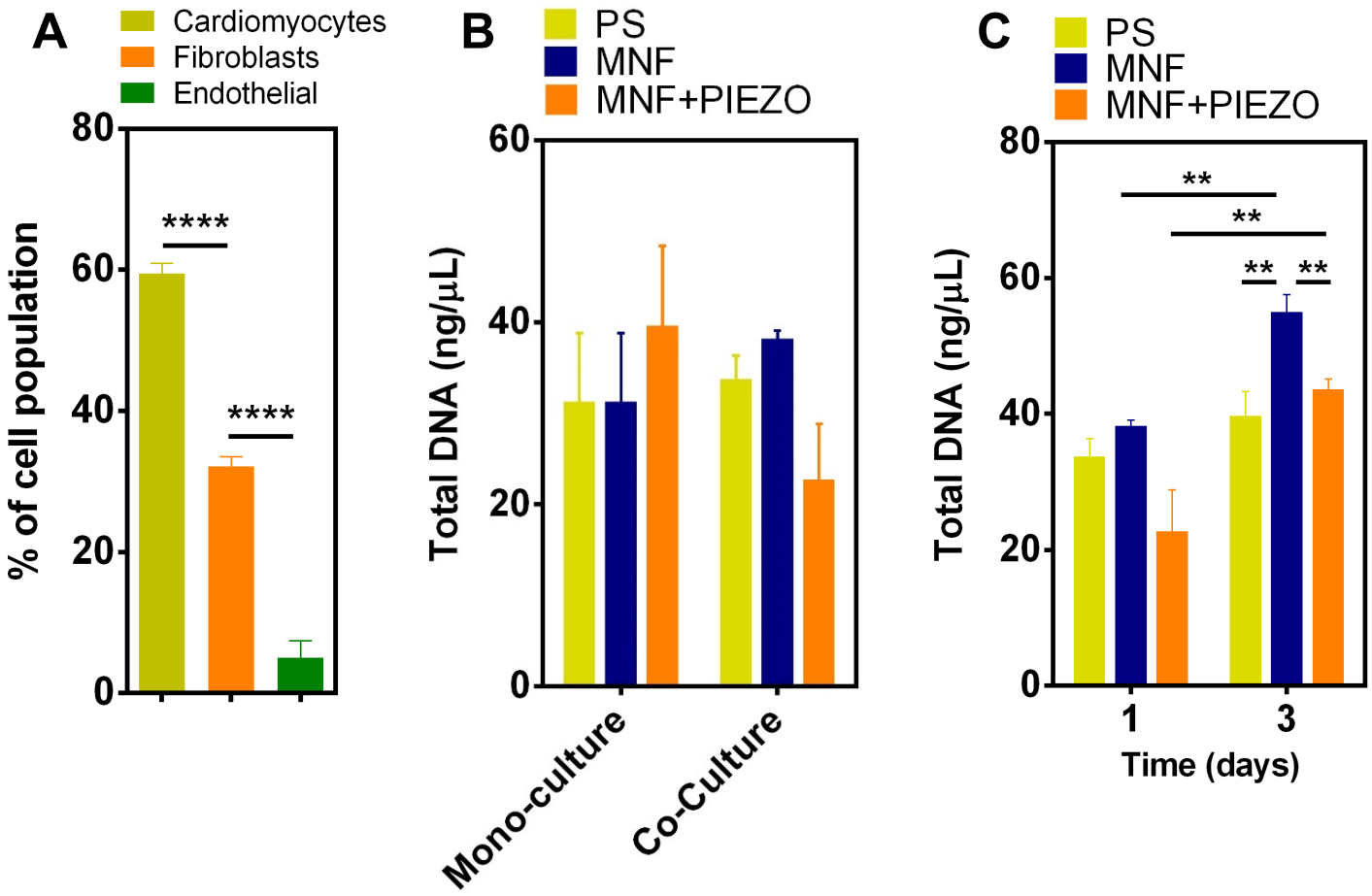

Supplementary Fig. 3 - Cardiac cell composition, adhesion and proliferation in the different substrates. (A) Rat fetal cardiac cells after isolation were characterized by FACS. Cells were fixed with a 4% paraformaldehyde solution and then permeabilized with saponin. Afterwards each population was marked with different fluorescence markers targeting a specific subpopulation of the cardiac tissue: anti-vimentin for cardiac fibroblasts, anti-α-actinin for cardiomyocytes and anti-CD31 for endothelial cells. **(B)** Cardiac cell adhesion to the different substrates. Purified (mono-culture; CMs: ≃ 95%) and non-purified cells (co-culture; CMs: ≃ 60%; fibroblasts: ≃ 30%; endothelial cells: ≃10%) were cultured in the different substrates for 3 days. Cells were lysed at days 1 and 3 and total DNA quantified. **(C)** Cardiac cell proliferation. Purified (mono-culture) and non-purified (co-culture) cells were cultured in the different substrates for 3 days. Cells were lysed at days 1 and 3 and total DNA quantified. In A, B and C, results are Average ± SEM, n=4. * denotes statistical significance: **P<0.01, ****P<0.0001.

Supplementary Figure 4

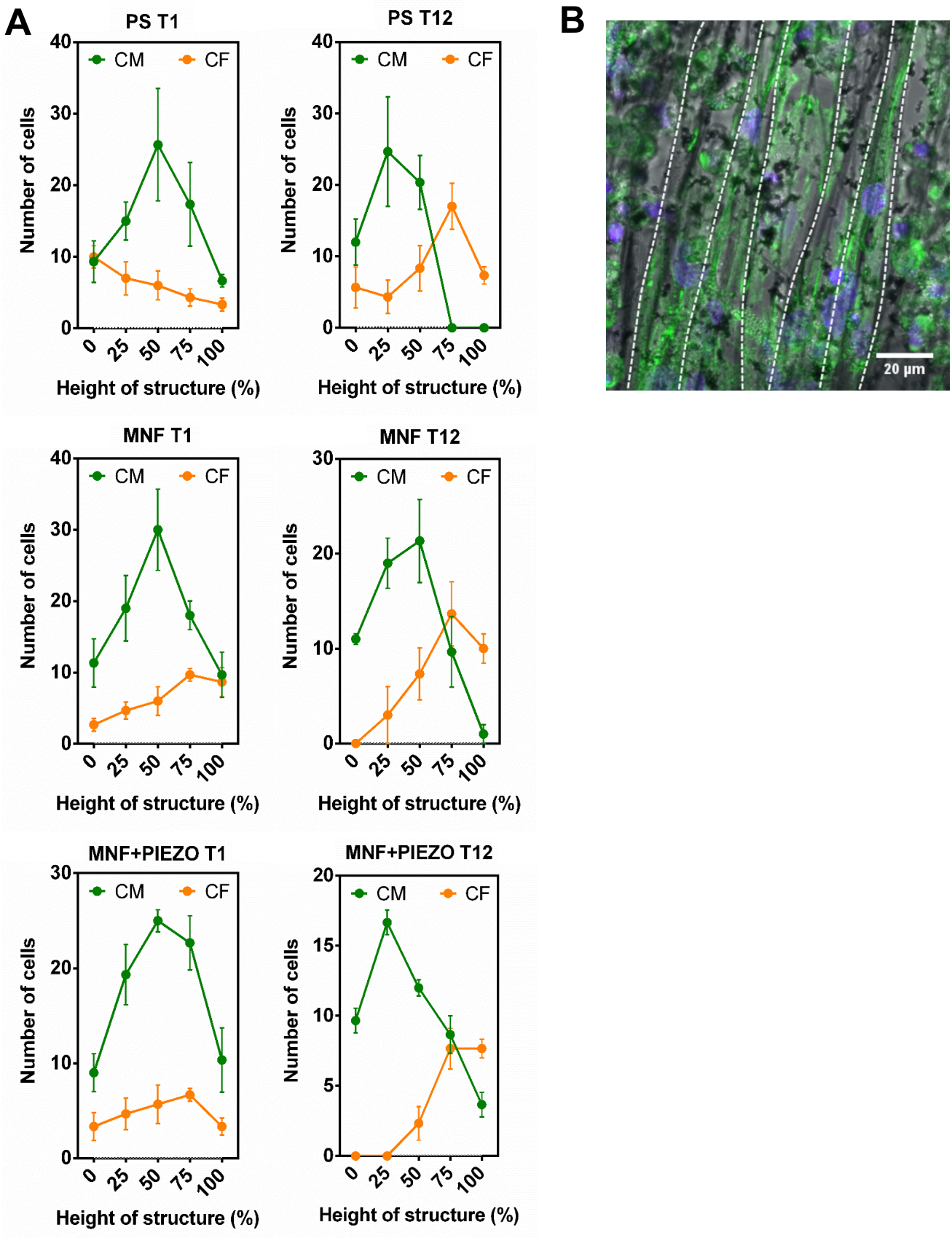

Supplementary Fig. 4 - Spatial distribution of CMs and CFs in the scaffold. (A) Total number of cells was assessed in the Z-stacks obtained by confocal microscopy. CMs and CFs were monitored by the expression of α-actinin and vimentin, respectively. Total height of structures was expressed in percentage to account for differences between the height of the structures. Results are Average ± SEM, n=3, 3 replicas per experimental group. **(B)** Representative confocal image showing direct interaction of CMs with PIEZO microfibers (in dash). Scale bar is 20 µm.

Supplementary Figure 5

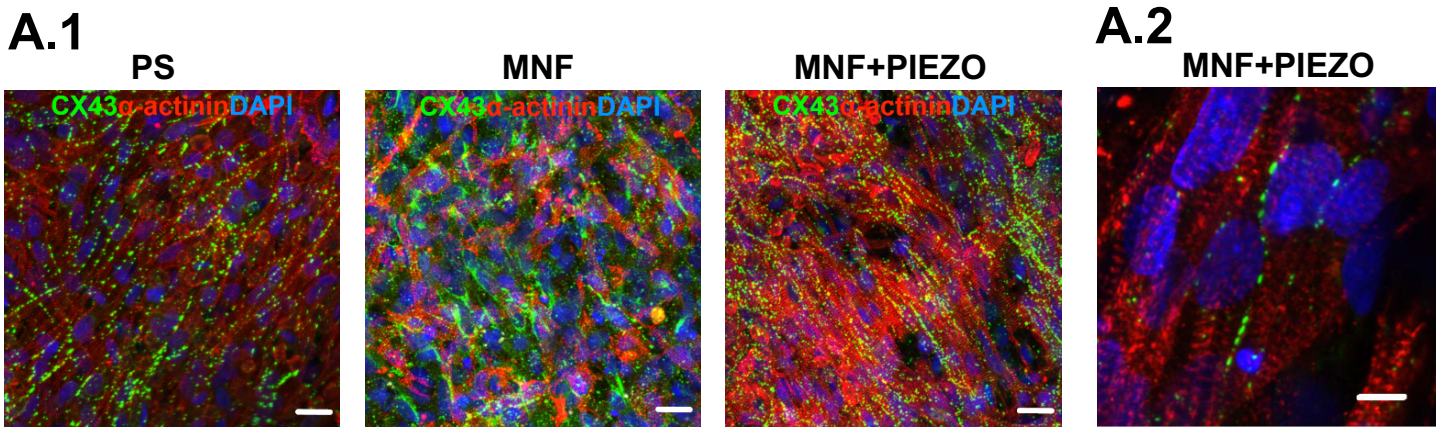

Supplementary Fig. 5 - Expression of Cx43 (total protein) and sarcomeric α-actinin in rat CMs. (A.1) Confocal microscope images of prenatal rat cardiac cells cultured in PS, MNF or MNF +PIEZO for 12 days. Images show the expression and localization of total Cx43 and sarcomeric α-actinin. Scale bar represents 20 μm. **(A.2)** Magnification of CMs cultured on MNF+PIEZO showing Cx43-mediated CM-CM junctions. Scale bar represents 5 μm. In all images, green is Cx43, red is α-actinin and blue is cell nuclei as stained by DAPI.

Supplementary Figure 6

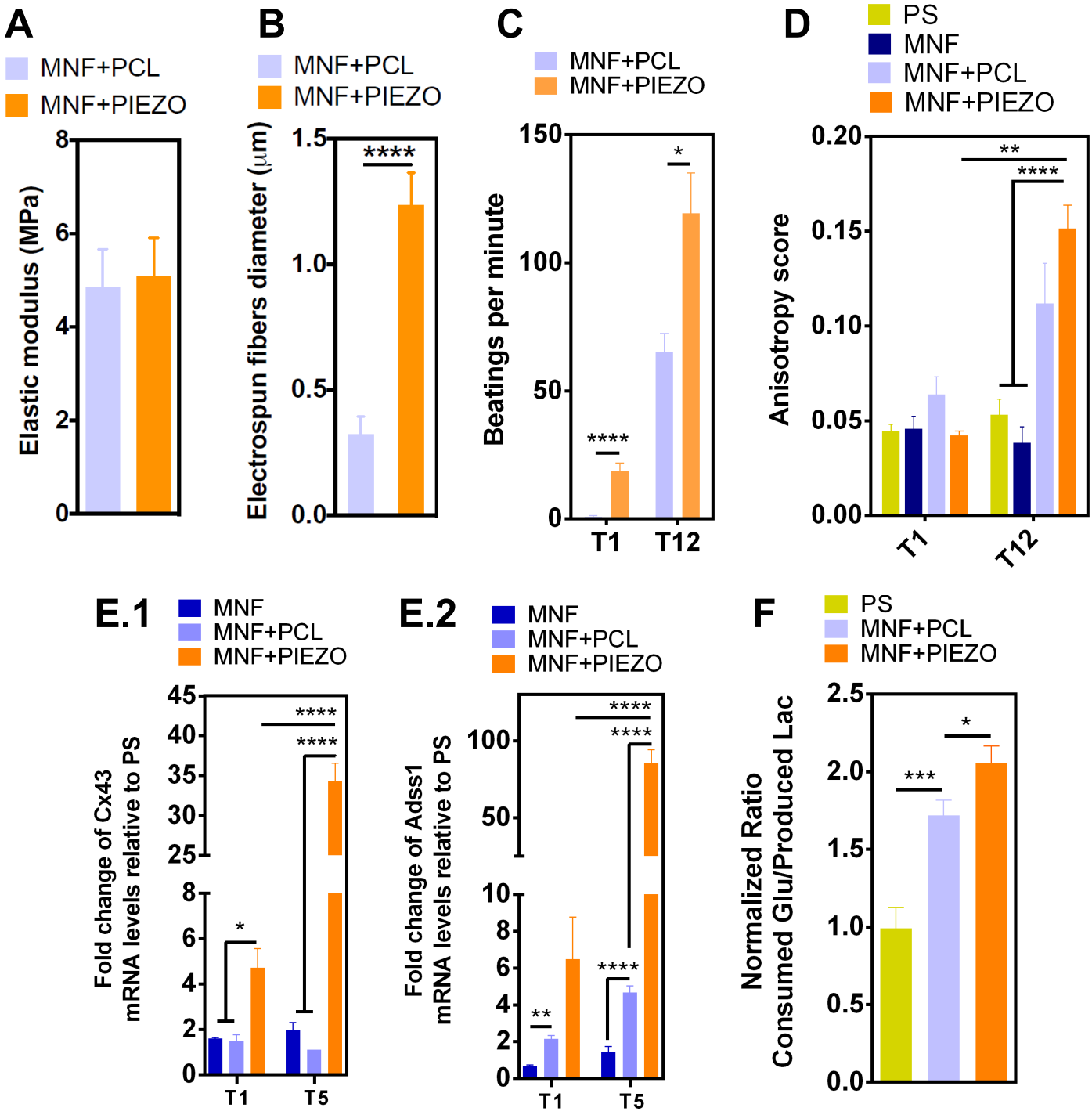

Supplementary Fig. 6 - Properties of MNF+PCL fiber scaffolds and impact on rat cardiac cells. (A) Elastic modulus. **(B)** Diameter of electrospun fibers. **(C)** Beatings of CMs seeded in MNF+PCL or MNF+PIEZO scaffolds at days 1 and 12. **(D)** CM alignment in different substrates. The alignment was calculated through confocal microscopy images (objective 63x) of immunostained samples. CMs were positive for α-actinin while CFs were positive for vimentin. Cellular alignment was quantified by taking account the deviation (20º degrees) towards a common reference line. **(E)** Cellular expression of Cx43 (E.1) and muscle-specific isoform of adenylosuccinate synthetase (Adss1) (E.2) as evaluated by qRT-PCR. Rat cardiac cells were cultured on MNF, MNF+PCL, MNF+PIEZO scaffolds and mRNA expression levels was evaluated after 1 and 5 days of culture. Target genes were normalized against TBP gene expression. **(F)** Ratio of glucose consumption and lactate production in cells cultured in scaffolds containing electroactive (MNF+PIEZO) and non-electroactive fibers (MNF+PCL). The results were normalized by cells cultured in PS. In A-C, results are Average ± SEM, n=4. In D, results are Average ± SEM, n=3 (three independent experiments; each experiment having 3 technical replicates). In E and F results are Average ± SEM, n=2 (two independent experiments; having E 6 technical replicates and F 12 technical replicates). *Denotes statistical significance: *P<0.05, **P<0.01, ***P<0.001, ****P<0.0001.

Supplementary Figure 7

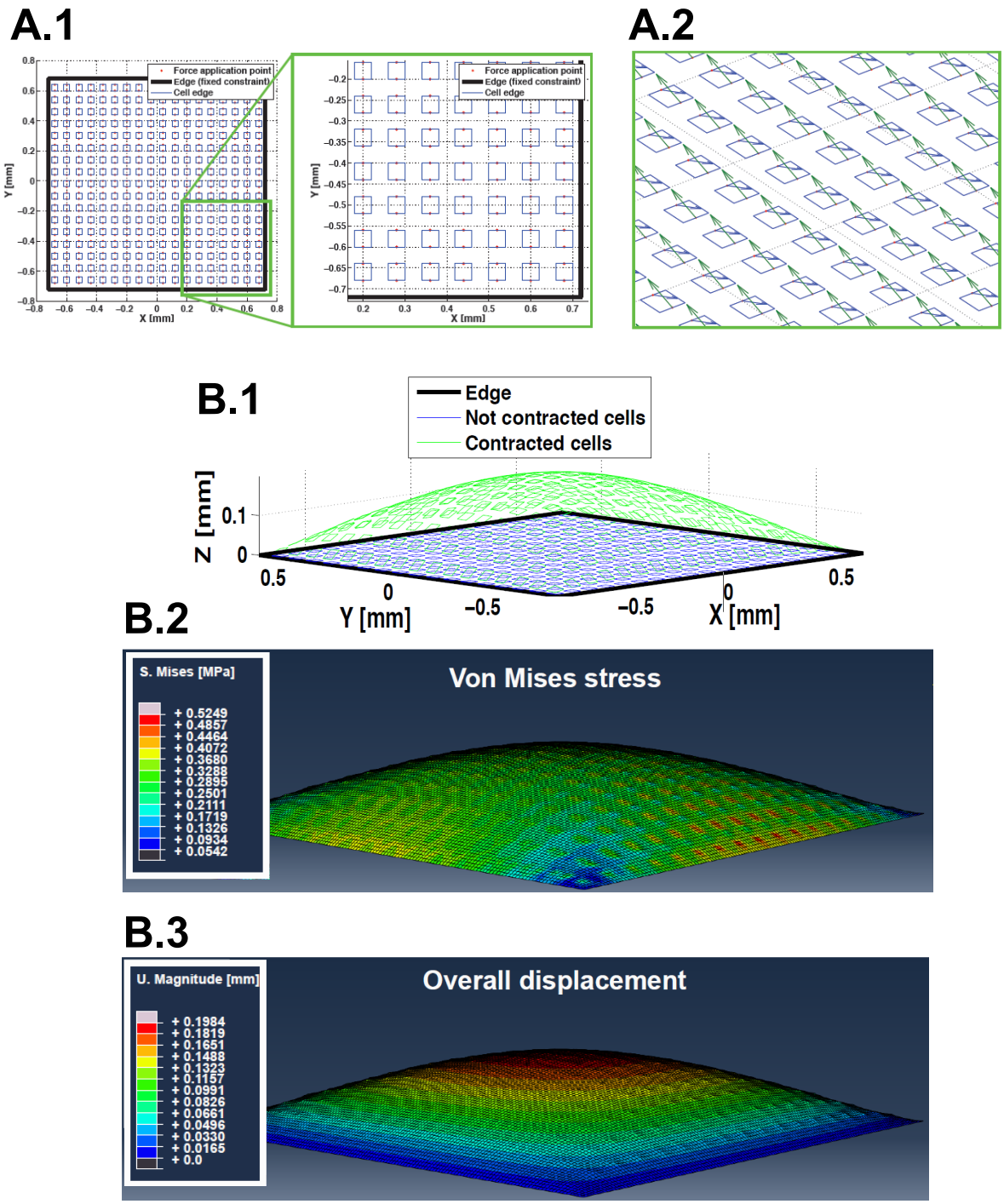

Supplementary Fig. 7 - FEM simulations of scaffold deformation under CM contraction. (A) Substrate model, a 1,4x1,4 mm^2 membrane, parametrically designed in the Matlab environment and implemented in the Abaqus simulation environment. Simulation conditions included values for thickness and elastic modulus of the membrane imported from MNF+PIEZO experimental data. Cell dimensions and distribution (A1) were extracted from fluorescence image analysis, while the imposed cell contraction force and the angle between (A2) the contraction force vectors and the substrate surface derived from literature data (Feinberg *et al*, 2007; Carisey *et al* 2013; Iskratsch *et al* 2014). **(B)** 3D representations of simulated deformation under the influence of beating cells. (B1) Deformation displacement in the absence and presence of CM contraction; (B2) von Mises stress (MPa) distribution over the surface of the simulated layer while under CM beating denotes a generally elastic deformation occurs during this process; (B.3) Scalar representation of surface point displacement (in mm) demonstrates higher shifts in the central region of the surface during CM induced deformation.